Phosphodiesterase 1A physically interacts with YTHDF2 and reinforces the progression of non-small cell lung cancer

Chong Zhang[1,2#], Zuoyan Zhang[2,3,4#], Yuchen Wu[5#], Jing Cheng[2,7], Kaizhi Luo[2,6], Zhidi Li[2,7], Manman Zhang[2,7], Jian Wang[1]*, Yangling Li[8]*

[1]Department of oncology, Shangyu People's Hospital of Shaoxing, Shaoxing, Zhejiang, China, 312300

[2]Department of Pharmacy, School of Medicine, Hangzhou City University, Hangzhou, Zhejiang, China, 310015

[3]Department of Pharmacy, Ningbo First Hospital, Ningbo, China, 315010

[4]Department of Pharmacy, The Affiliated Hospital of Northwest University · XI'AN NO.3 Hospital, Shanxi, China, 710038

[5]Department of Clinical Medicine, The First School of Medicine, Wenzhou Medical University, Wenzhou, Zhejiang, 325035

[6]Department of Pharmacy, Zhejiang University of Technology, Hangzhou, Zhejiang, China, 310027

[7]College of Pharmaceutical Sciences, Zhejiang University, Hangzhou, Zhejiang, China, 310058

[8]Department of Clinical Pharmacology, Key Laboratory of Clinical Cancer Pharmacology and Toxicology Research of Zhejiang Province, Affiliated Hangzhou First People’s Hospital, Zhejiang University School of Medicine, Hangzhou, Zhejiang, China, 310006

[#]Chong Zhang, Zuoyan Zhang, and Yucheng Wu contributed equally to this work

[*] **Correspondence should be addressed to:** Yang ling Li and Jian Wang;

Address: School of Medicine, Hangzhou City University, No.51 Huzhou Street, Hangzhou, Zhejiang, China, 310015 and Department of Clinical Pharmacology, Affiliated Hangzhou First People's Hospital, Zhejiang University School of Medicine, No.261 Huansha Road, Hangzhou, Zhejiang, China, 310006;

E-mail: liyangling1215@163.com and 2538765918@qq.com;

Tel.: 86-0571-88283821, Fax: 86-0571-88283821.

Abstract

Non-small cell lung cancer (NSCLC) is the most common subtype of lung cancer, and the prognosis is poor due to distant metastasis and drug resistance. Thus, there is an urgent need to discover novel therapeutic targets and strategies to overcome cisplatin resistance and metastasis. A series of in vitro and in vivo phenotype experiments were performed to investigate the role of PDE1A in NSCLC. The RIP assay, mRNA stability assay and LC-MS/MS were performed to investigate the molecular mechanisms of PDE1A in NSCLC progression. We demonstrated that phosphodiesterase 1A (PDE1A) promoted metastasis and EMT progression of NSCLC. In addition, NSCLC cells overexpressing PDE1A promoted angiogenesis by regulating exosome release. IL-6/JAK/STAT3 signaling pathway was highly enriched in PDE1A-coexpresssed genes, and PDE1A promoted NSCLC metastasis by activating the STAT3 pathway. GO enrichment analysis of PDE1A-interacting genes showed that PDE1A might interact with YTHDF2 and participate in m6A-containing RNA binding. The binding between PDE1A and YTHDF2 was verified, and PDE1A regulated the STAT3 pathway by interacting with YTHDF2. The mechanism of YTHDF2/PDE1A complex in regulating STAT3 pathway was predicted by overlapping YTHDF2-interacting-RNAs, and genes coexpressed with YTHDF2 and STAT3. The interactions between YTHDF2 and target mRNAs were predicted, and there were three predicted targets of YTHDF2 with high scores: NRF2, SOCS2, and MET. Indeed, PDE1A

interacted with YTHDF2, destabilized SOCS2, and activated STAT3 pathway. Moreover, PDE1A suppression sensitized anti-NSCLC activity of cisplatin via regulating NRF2 and MET. This work not only uncovers a novel PDE1A/YTHDF2/STAT3 pathway in NSCLC progression but also provides therapeutic strategies for treating NSCLC patients with metastasis or cisplatin-resistance.

Key word: PDE1A; metastasis; cisplatin resistance; YTHDF2; NSCLC; STAT3

Introduction

Lung cancer is one of the most frequently diagnosed cancers and the leading cause of cancer-related mortality worldwide [1]. Non-small cell lung cancer (NSCLC) represents approximately 85% of lung cancers and is the most common subtype of lung cancer [2]. Despite rapid advances in the clinical treatment of NSCLC in recent years, the prognosis of NSCLC patients is still poor due to recurrence and distant metastasis [3]. Cisplatin-based chemotherapy is the first-line treatment for the majority of metastatic NSCLC cases, but drug resistance develops rapidly [4, 5]. However, the mechanisms of cisplatin resistance and NSCLC metastasis are still poorly understood.

Phosphodiesterases (PDEs) are a class of enzymes that hydrolyse cyclic adenosine monophosphate (cAMP) and cyclic guanosine monophosphate (cGMP), reducing the signaling of these important intracellular second messengers [6]. PDEs consist of 11 family members, and each family member contains multiple subtypes [7]. PDEs are being pursued as therapeutic targets in multiple diseases, including the cardiovascular system, metabolism, pulmonary system, nervous system, immunity, and cancers [8]. For example, PDE3 inhibitors are used to treat heart failure and peripheral artery disease, and PDE4 inhibitors are approved to treat inflammatory diseases [9]. Multiple studies have shown that PDEs, such as PDE4 and PDE5, play a vital role in the progression of tumors and are regarded as potential therapeutic targets for cancer treatment [9, 10]. The PDE1 family

member has three subtypes, including PDE1A, PDE1B and PDE1C, with different affinities for cAMP and cGMP [11]. The effect and mechanism of PDE1 in regulating cancer progression remain elusive.

N^6-methyladenosine (m^6A) is the most abundant RNA modification, and the process of m^6A modification is reversible: m6A is installed by “writers”, removed by “erasers”, and recognized by “readers” [12]. YT521-B homology domain family member 2 (YTHDF2), belonging to the YTH domain protein family, has been validated as m^6A “reader” and regulates the stability of messenger RNAs (mRNAs) [13]. YTHDF2 promotes the progression of lung adenocarcinoma by recognizing m6A modification and influencing mRNA fate [14]. Furthermore, YTHDF2 orchestrates the reprogramming of tumor-associated macrophages in the tumor microenvironment (TME), and YTHDF2 is an effective target to enhance cancer immunotherapy [15]. In this study, we first demonstrated that PDE1A promoted NSCLC metastasis and cisplatin resistance via interacting with YTHDF2.

Materials and methods

Materials

Vinpocetine (V107535) was purchased from Aladdin (Shanghai, China). Cisplatin (S1166), SH-4-54 (S7337), SQ22536 (S8283), and GW4869 (S7609) were obtained from Selleck Chemicals (Houston, TX, USA). Antibodies against β-actin (SC-1616), GAPDH (SC-25778), MET (SC-514148), and caspase-3 (SC-7148) were obtained from Santa Cruz Biotechnology (Dallas,

Texas, USA). Antibodies against N-cadherin (14215), STAT3 (9139), p-STAT3 (Y-705) (9145), p-Met (Tyr1234) (3077), cleaved-PARP (9541), Vimentin (5741), JAK2 (3230S), and NRF2 (12721) were obtained from Cell Signaling Technology (Danvers, MA, USA). An antibody against α-tubulin (AT7819) was purchased from Beyotime Biotechnology (Shanghai, China). Antibodies against PDE1A (12442-2-AP), YTHDF2 (24744-1-AP), lamin B (12595-1-AP), and E-cadherin (20874-1-AP) were obtained from Proteintech (Rosemont, IL, USA).

Cell lines and cell culture

Human NSCLC cell lines (A549, NCI-H1299, and NCI-H460), a bronchial epithelial cell line (HELF), and umbilical vein endothelial cells (HUVECs) were maintained in RPMI-1640 medium supplemented with 10% fetal bovine serum (FBS) and 100 U/ml penicillin/streptomycin. All the cell lines were purchased from the Shanghai Institute of Biochemistry and Cell Biology (Shanghai, China), cultured at 37 °C with 5% CO_2 and confirmed to be mycoplasma-free.

siRNA transfection

Scramble siRNA, siPDE1A, siPDE1B, siPDE1C, siSTAT3, and siYTHDF2 were synthesized by GenePharma (Suzhou, China). Then, NSCLC cells were transfected with siRNA (40 nM) using PolyPlus-transfection reagent in accordance with the instructions. The sequences of siRNAs are summarized in Table S1.

Sulforhodamine B (SRB) assay

NSCLC cells were treated with the indicated compounds, and subsequently fixed with ice-cold TCA and stained with 0.4% SRB (w/v) solution. Cell proliferation was determined by SRB assay according to previously reported methods [16].

Wound healing assay

NSCLC cells were seeded on a 24-well plate and cultured as a monolayer to 90% confluence. The monolayer was scratched with a 10 μL pipette tip, and then the cells were cultured with FBS-free culture medium for 24 h. Images of the wounded cell monolayer were taken using a microscope (Olympus, Japan) at 0 h and 24 h. The wound closure rate was calculated as follows: $(G_0-G_{24}) / G_0 \times 100\%$, where G_0 and G_{24} represent the gap areas at 0 and 24 h, respectively.

Migration and invasion assays using transwells

Migration and invasion assays were performed using a 24-well transwell chamber system (pore size: 8 μm, Corning, USA). A total of 5×10^4 cells were seeded in the upper chamber of an insert with 0.4 ml serum-free culture media in 24-well plates. Then, 0.6 ml culture medium with 20% FBS was added to the lower chamber. For invasion assays, the upper transwell chamber of the insert was coated with Matrigel (BD Biosciences, Bedford, MA, USA) before plating cells. After incubation for 24 h, migratory or invasive cells were stained with 0.5% crystal violet and analyzed under a light microscope.

Protein extraction and western blotting analysis

Briefly, cells were washed three times with cold PBS and pelleted. The pellet was resuspended in lysis buffer, incubated on ice with frequent vortex for 30 min, and the lysate was obtained by centrifugation at 12000 rpm for 30 min. Proteins were fractionated by SDS-PAGE, transferred onto PVDF membranes, blocked in 5% nonfat milk in PBS/Tween-20, and then blotted with specific primary antibody overnight at 4 °C, followed by incubation with secondary antibody for 1 h at room temperature. Bands were detected by the Odyssey CLX Image Studio system (version 5.0.21, LiCor Odyssey, LI-COR Biosciences).

Immunoprecipitation and LC-MS/MS

For coimmunoprecipitation, the cells were lysed with IP buffer and centrifuged at 10000 × g for 30 min at 4 °C. The cell lysates were treated with protein G magnetic beads at 4 °C for 1 h. Subsequent immunoprecipitation reactions were set up with equal quantities of the lysates. Primary antibody was added to the lysate, and the mixture was incubated overnight with slow shaking at 4 °C, and then incubated with protein G magnetic beads at 4 °C for 1 h. Subsequently, the lysates were centrifuged at 3000 g at 4 °C for 5 min. We aspirated the supernatant, washed the protein G magnetic beads with lysis buffer 3-4 times, and detected by SDS-PAGE or LC-MS/MS (Micrometer Biotech Company, Hangzhou, China).

Extraction of RNA and quantitative real-time PCR (qRT-PCR)

Total RNA was extracted from cells by utilizing TRIzol™ Reagent (Invitrogen, Thermo Fisher Scientific). RNA was reverse-transcribed into cDNA using an iScript cDNA Synthesis kit (Bio-Rad, Hercules, CA, USA). qRT-PCR was performed using the PerfectStart Green qPCR SuperMix kit (TransGen Biotech, Beijing, China). The levels of mRNA were analyzed by the Bio-Rad CFX96 real-time PCR system (Bio-Rad, Hercules, CA, USA). GAPDH was used as an endogenous control for mRNA qualification and the 2-ΔΔCt method was applied to calculate the relative expression. The primers used are listed in Table S2.

RNA binding protein immunoprecipitation (RIP)

RIP assays were performed using a Magna RIP Kit (17-701, Millipore, MA, USA) following the manufacturer's instructions. In brief, magnetic beads precoated with 5 mg normal antibodies against PDE1A/YTHDF2 or rabbit IgG (Millipore) were incubated with cell lysates at 4 °C overnight. The beads containing immunoprecipitated RNA-protein complexs were treated with proteinase K to remove proteins. Then RNAs of interest were purified with TRIzol and measured by qRT-PCR.

Plasmid and shRNA transfection and infection

Two micrograms of overexpressing plasmid or shRNA of the indicated genes was transfected into cells using PolyPlus-transfection reagent. For shRNA used in lentivirus-mediated interference, complementary sense and antisense oligonucleotides encoding shRNAs targeting PDE1A were synthesized,

annealed, and cloned into pLKO.TRC vector (Addgene, 10878). The PDE1A-FLAG overexpression plasmid was synthesized by GenScript (Nanjing, Jiangsu, China). YTHDF2-HA expression plasmids were synthesized via cloning YTHDF2 with an HA tag into the pcDNA3.1(-) vector.

In vivo animal experiment

Female nude mice (BALB/c, 4-6 weeks old) were obtained from Shanghai SLAC Laboratory Animal Co., Ltd. A total of 2×10^6 NCI-H1299 cells transfected with shPDE1A/control shRNA or PDE1A overexpressing plasmid/empty vector were suspended in 0.1 ml of PBS and injected into mice via the tail vein. After 60 days, the mice were sacrificed, and the lung tissues were collected to observe pulmonary nodules. The lung, liver, kidney, pancreas, and other tissues were separated, fixed in 4% paraformaldehyde, and stained using H&E. All procedures were approved by the Institutional Animal Care and Use Committee of Zhejiang University City College (No. 22001).

mRNA stability assay

NSCLC cells were seeded in six-well plates and grown to approximately 30% confluence followed by siRNA transfection and incubation for 24 h. Then, cells were incubated with actinomycin D (5 μg/ml) for 0, 3 or 6 h followed by RNA extraction. The half-life of mRNA was analyzed by qRT-PCR. The mRNA expression for each group at the indicated time was calculated and normalized to GAPDH.

Statistical analysis

Data are presented as the mean ± SD from 3 independent experiments. Two-tailed Student's t test was used to compare 2 groups. P values < 0.05 were considered significant. *P < 0.05; **P < 0.01; ***P < 0.001.

Results

PDE1A overexpression predicts a poor prognosis in lung cancer patients

First, we found that PDE1A was highly expressed in lung cancer compared with normal lung tissue using immunohistochemistry (Figure 1A and Figure S1) [17, 18]. As shown in Figure 1B, overexpression of PDE1A was also observed in three NSCLC cell lines compared with normal human lung fibroblasts (HELF cells). Additionally, the overexpression of PDE1A was also observed in lung cancer from high-risk patients compared with low-risk patients (p<0.0001, Figure 1C), and lung cancer patients in the high-risk group had shorter survival times than those in the low-risk group (Figure 1D) [19, 20]. Furthermore, lung cancer patients with high levels of PDE1A in their tumors had shorter overall survival than those with low PDE1A expression, indicating that PDE1A overexpression was correlated with a poor prognosis in lung cancer patients (Figure 1E) [21, 22]. Thus, PDE1A might be a novel prognostic predictor in lung cancer treatment and contribute to lung cancer progression.

PDE1A promotes the metastasis and EMT of NSCLC cells both *in vitro*

239 **and *in vivo***

240 To investigate the biological function of PDE1A in lung cancer development,
241 gene set enrichment analysis (GSEA) and overrepresentation enrichment
242 analysis (ORA) were performed to analyze the biological process of PDE1A in
243 NSCLC using LinkedOmics [23]. As shown in Figure S2A, PDE1A might be
244 involved in the adhesion, migration, and motility of NSCLC cells, which are
245 critical parameters in the metastatic dissemination of cancer cells. Tumor
246 angiogenesis, the recruitment of new blood vessels, enables a pre-existing
247 tumor to grow and metastasize [24]. PDE1A might also participate in
248 mesenchyme development, angiogenesis, vasculature development, cellular
249 response to VEGF stimulus, blood vessel morphogenesis and development
250 (Figure S2A-C). Thus, we hypothesized that PDE1A might promote the
251 metastatic potential of NSCLC cells.

252 First, PDE1A silencing did not cause a significant decrease in the proliferation
253 of NSCLC cells relative to that in the control siRNA group (Figure S3A).
254 Moreover, PDE1A overexpression had no significant effect on the proliferation
255 of NSCLC cells (Figure S3B). As bioinformatics analysis demonstrated that
256 PDE1A might promote the metastatic potential of NSCLC cells, wound healing
257 and transwell assays were used to investigate the migration and invasion
258 capacity of PDE1 family members. Knockdown of PDE1 family members
259 suppressed the migratory ability of NCI-H1299 cells, and siPDE1A exerted a
260 stronger suppression effect on the migration of NCI-H1299 cells than

261 siPDE1B and siPDE1C transfection (Figure S4A). Meanwhile, siPDE1A
262 resulted in more profound suppression of EMT progression in NCI-H1299
263 cells than siPDE1B and siPDE1C transfection (Figure S4B). Thus, PDE1
264 family members, particularly PDE1A, might be involved in the metastatic
265 behavior of NSCLC cells.
266 As shown in Figure 2A and 2B, suppression of PDE1A markedly reduced the
267 migratory and invasive capacity of NSCLC cell lines, and the wound healing
268 assay also showed that NSCLC cells with PDE1A knockdown had a slower
269 wound closure rate than control siRNA-transfected cells (Figure 2C and 2D).
270 Furthermore, PDE1A knockdown increased E-cadherin expression and
271 reduced N-cadherin expression, indicating that PDE1A silencing suppressed
272 EMT progression in NSCLC cells (Figure 2E). Meanwhile, the PDE1 inhibitor
273 vinpocetine significantly suppressed the migration and EMT of NSCLC cells
274 (Figure 2F - H). To determine the effects of PDE1A on NSCLC cell migration
275 and invasion *in vivo*, nude mouse models were established using PDE1A-
276 shRNA- and control-shRNA-treated NCI-H1299 cells. As shown in Figure 2I
277 and Figure S4C, the number of pulmonary metastatic nodules was decreased
278 in the PDE1A-shRNA group compared with the control-shRNA group in nude
279 mice.
280 In contrast, PDE1A overexpression significantly enhanced the migratory and
281 invasive capacities of NSCLC cells (Figure 3A and 3B). In addition, NSCLC
282 cells with high PDE1A expression had a higher wound closure rate than those

283 transfected with empty vector (Figure 3C). Meanwhile, PDE1A overexpression
284 decreased E-cadherin expression and elevated N-cadherin expression,
285 indicating that PDE1A promoted EMT progression of NSCLC cells (Figure
286 3D). To compare the expression of PDE1A in NSCLC cells with high and low
287 invasive potential, we established series of NSCLC cell lines with differential
288 invasive abilities through multiple selections using a transwell chamber assay
289 (Figure 3E, Figure S5A and S5B). The protein and mRNA levels of PDE1A
290 were higher in highly invasive NSCLC cells than in NSCLC cells with low
291 invasive potential (Figure 3F and 3G). In an *in vivo* nude mouse experiment,
292 NSCLC cells overexpressing PDE1A produced more pulmonary metastatic
293 nodules than the parental NSCLC cells (Figure 3H and Figure S5C).

294 **NSCLC cells overexpressing PDE1A promote angiogenesis in the TME**

295 GSEA demonstrated that PDE1A expression was positively correlated with
296 angiogenesis in lung cancer (Figure 4A). Thus, we constructed a tumor
297 microenvironment by coculturing NSCLC cells with vascular endothelial cells
298 (Figure 4B). NSCLC cells overexpressing PDE1A promoted the migration of
299 HUVECs, and NSCLC cells with low levels of PDE1A suppressed the
300 migration of HUVECs (Figure 4C and 4D). Next, we treated NSCLC cells with
301 GW4869 to reduce exosome release and found that GW4869 suppressed the
302 enhancement of the migratory ability of HUVECs induced by NSCLC cells
303 overexpressing PDE1A (Figure 4E). Meanwhile, compared with negative
304 control, shPDE1A significantly suppressed tumor angiogenesis of NSCLC *in*

305 *vivo* (Figure 4F). Thus, NSCLC cells overexpressing PDE1A promote
306 angiogenesis in the TME.

307 **PDE1A promotes the metastasis of NSCLC cells via the STAT3 signaling**
308 **pathway**

309 Then, we investigated whether PDE1A-enhanced metastasis was dependent
310 on cAMP metabolism activity. As shown in Figure S6A, the cAMP inhibitor
311 SQ22536 failed to rescue the migrative ability suppressed by siPDE1A in
312 NSCLC cells, indicating that the basic molecular function might not be
313 involved in the metastasis of PDE1A. To better explore the mechanism of
314 PDE1A in NSCLC progression, we performed bioinformatic analysis of PDE1A
315 coexpressed genes, which revealed that PDE1A might be involved in the
316 JAK/STAT3, Hedgehog, and TGF-β pathways in NSCLC (Figure 5A).
317 Meanwhile, GSEA enrichment analysis demonstrated that PDE1A might
318 participate in IL-6 production (Figure 5B), thus we hypothesized that IL-
319 6/JAK/STAT3 signaling might be involved in PDE1A-promoted metastasis in
320 NSCLC. As shown in Figure 5C, PDE1A overexpression increased the
321 phosphorylation level of STAT3 in NSCLC cells. In contrast, PDE1A
322 knockdown or the PDE1 inhibitor vinpocetine suppressed the phosphorylation
323 of STAT3 in NSCLC cells (Figure 5D and 5E). Moreover, STAT3 suppression
324 by siRNA or SH-4-54 significantly reversed the enhancement of NSCLC cell
325 migration induced by PDE1A overexpression (Figure 5F and 5G). In addition,
326 the suppression of STAT3 inhibited PDE1A-induced EMT progression in

327 NSCLC cells (Figure 5H and 5I). Thus, PDE1A promoted the metastasis of
328 NSCLC cells via activating the STAT3 signaling pathway, but the direct
329 interaction between PDE1A and STAT3 could not be observed in NSCLC cells
330 (Figure 5J). Moreover, PDE1A was mainly overexpressed in the cytoplasm in
331 NSCLC cells (Figure 5K), and we next further explored the mechanism by
332 which PDE1A in promotes the STAT3 signaling pathway in the cytoplasm.

333 **PDE1A physically interacts with YTHDF2 and promotes the metastasis**
334 **of NSCLC cells**

335 To investigate the mechanism by which PDE1A promotes NSCLC metastasis
336 and activates the STAT3 pathway, the proteins interacting with PDE1A in
337 NSCLC were determined using immunoprecipitation followed by mass
338 spectrometry analysis (Table S3). To identify the key proteins involved in
339 PDE1A-mediated STAT3 activation, we generated a Venn diagram, which
340 showed that there were 9 overlapping genes among those coexpressed with
341 STAT3 in NSCLC clinical samples, PDE1A-interacting proteins, and
342 overexpressed in NSCLC compared with normal tissues (Figure 6A).
343 Meanwhile, GO enrichment analysis of PDE1A interacting genes was used to
344 predict the molecular function of PDE1A, and PDE1A might participate in
345 m6A-containing RNA binding in NSCLC progression (Figure 6B). Thus, we
346 hypothesized that PDE1A might interact with YTHDF2 and participate in m6A-
347 containing RNA binding during NSCLC progression. The physical binding
348 between PDE1A and YTHDF2 was confirmed by silver staining and

349 immunoprecipitation (Figure 6C and 6D). Furthermore, YTHDF2 knockdown
350 reversed the enhancement of NSCLC migration induced by PDE1A
351 overexpression, indicating that PDE1A might interact with YTHDF2 and
352 promote the metastasis of NSCLC (Figure 6E and Figure S6B and S6C). The
353 mRNA and protein levels of YTHDF2 were upregulated in NSCLC compared
354 with normal lung tissues (Figure S7A and S7B) [25]. In addition, YTHDF2
355 overexpression predicted poor outcomes in lung cancer patients (Figure S7C)
356 [21, 22]. Meanwhile, the activation of STAT3 by PDE1A could be reversed by
357 YTHDF2 knockdown in NSCLC cells (Figure 6F). Furthermore, PDE1A was
358 positively correlated with YTHDF2 expression with a Pearson correlation
359 coefficient above 0.3 in NSCLC tissues (Figure 6G) [25]. Thus, PDE1A might
360 regulate the STAT3 signaling pathway via interacting with YTHDF2.

361 **PDE1A interacts with YTHDF2 to regulate the SOCS2/STAT3 signaling**
362 **pathway**

363 To gain mechanistic insights regarding the key target mRNA by which the
364 PDE1A/YTHDF2 complex regulates the STAT3 signaling pathway, we
365 generated a Venn diagram, which showed that there were 33 overlapping
366 genes among RNAs that physically interact with YTHDF2, YTHDF2-
367 coexpressed genes, and STAT3-coexpressed genes in lung cancer (Figure 7A
368 and Table S4) [26-29]. Then, the interactions between the YTHDF2 protein
369 and the mRNAs of 33 overlapping genes were predicted by RNA-Protein
370 Interaction Prediction online tool. There were three predicted targets of

371 YTHDF2 with high scores and highly correlated with STAT3 signaling as
372 previously reported, including NRF2, SOCS2, and MET (Table S5) [30]. SOCS
373 family members are cytokine-inducible negative regulators of the JAK/STAT
374 pathway, and SOCS2 suppresses the binding of JAK2 and STAT3, the activity
375 of JAK, and STAT3 activation [31]. Thus, we hypothesized that PDE1A might
376 interact with YTHDF2, influence the fate of SOCS2 mRNA, and regulate the
377 STAT3 signaling pathway in NSCLC cells. As shown in Figure 7B, the
378 interaction between YTHDF2 protein and SOCS2 mRNA was verified by RIP,
379 and we also proved the binding between PDE1A protein and SOCS2 mRNA
380 using RIP. Meanwhile, siPDE1A significantly enhanced the stability of SOCS2
381 mRNA in NSCLC cells (Figure 7C). Furthermore, YTHDF2 or PDE1A
382 negatively regulated the expression of SOCS2 mRNA in NSCLC cells, and
383 YTHDF2 overexpression successfully reversed the siPDE1A-induced SOCS2
384 mRNA accumulation. In contrast, siYTHDF2 enhanced siPDE1A-induced
385 SOCS2 mRNA accumulation (Figure 7D). These data indicated that YTHDF2
386 might negatively regulate the expression of SOCS2 mRNA via cooperating
387 with PDE1A.

388 **PDE1A suppression enhances the anti-NSCLC activity of cisplatin via**
389 **regulating MET and NRF2 expression**

390 As the PDE1A/ YTHDF2 complex might also regulate MET and NRF2, the
391 activation of MET or NRF2 triggers NSCLC resistance to chemotherapy, such
392 as cisplatin treatment [32, 33]. As shown in Figure 8A and 8B, siPDE1A

393 significantly suppressed the expression of MET and NRF2 compared with
394 control siRNA, and PDE1A overexpression enhanced the expression of MET
395 and NRF2 in NSCLC cells. Furthermore, vinpocetine restrained the
396 expression of MET and NRF2 in NSCLC cells (Figure 8C). These data
397 suggest that PDE1A could positively regulate MET and NRF2; thus, we
398 hypothesized that PDE1A might be involved in cisplatin resistance in NSCLC
399 cells. Indeed, PDE1A knockdown significantly enhanced the cytotoxicity of
400 cisplatin, and PDE1A overexpression decreased cisplatin-induced cytotoxicity
401 in NSCLC cells (Figure 8D and 8E). Meanwhile, vinpocetine plus cisplatin
402 synergistically suppressed the proliferation of NSCLC cells compared with
403 single agent treatment alone (Figure 8F). Furthermore, vinpocetine plus
404 cisplatin enhanced apoptosis induction in NSCLC cells compared with single
405 agent alone (Figure 8G). In addition, knockdown of PDE1A significantly
406 suppresses the mRNA level of MET and NRF2, and siYTHDF2 reversed the
407 activation of MET and NRF2 induced by PDE1A overexpression (Figure 8H
408 and 8I). These data indicate that PDE1A positively regulates MET and NRF2
409 via interacting with YTHDF2, and that PDE1A suppression enhances the anti-
410 NSCLC activity of cisplatin.

411 **Discussion**

412 NSCLC is becoming a leading cause of death globally due to its fast
413 progression and metastatic potential, and effective therapeutic targets are
414 urgently needed to block NSCLC metastasis [34]. PDEs are regarded as

415 therapeutic targets for multiple diseases, but the feasibility of targeting PDEs
416 to treat NSCLC metastasis may need further investigation [35]. In this study,
417 we showed for the first time that PDE1 promoted metastasis and EMT
418 progression in NSCLC cells. Furthermore, the expression of PDE1A was
419 closely correlated with the disease progression of NSCLC. These data first
420 indicated with PDE1A might be an efficacious therapeutic target for patients
421 with metastatic NSCLC.
422 The stimulation of the PDEs requires physiological concentrations of Ca^{2+} and
423 calmodulin, and Ca^{2+}/calmodulin-dependent cyclic nucleotide PDE1 is
424 involved in the communication between the cyclic nucleotide and Ca^{2+} second
425 messenger systems [36]. The increasing of Ca^{2+} in cancer cells stimulates
426 exosome biogenesis and release under both physiological and pathological
427 conditions [37, 38]. In this context, we assumed that PDE1A might be involved
428 in exosome biogenesis and release in NSCLC cells and play a vital role in
429 message communication in the TME. GSEA showed that PDE1A might be
430 involved in angiogenesis, vasculature development, and blood vessel
431 development. Indeed, NSCLC cells overexpressing PDE1A promoted
432 angiogenesis in the TME, and PDE1A knockdown significantly suppressed
433 angiogenesis of NSCLC *in vivo*. Furthermore, an exosome release inhibitor
434 successfully reversed the angiogenesis promoted by NSCLC cells
435 overexpressing PDE1A. Thus, this study first illustrated that PDEs might play
436 an important role in angiogenesis and the TME via regulating exosome

437 biogenesis and release in cancer cells.

438 During our attempt to reveal the downstream signaling pathway of PDE1A, we
439 found that the IL-6/JAK/STAT3 signaling pathway was highly enriched in
440 PDE1A coexpressed genes from NSCLC. Furthermore, PDE1A promoted the
441 metastasis of NSCLC cells via the STAT3 signaling pathway. Targeting the IL-
442 6/JAK/STAT3 signaling pathway is considered as a promising therapeutic
443 strategy for the management of NSCLC [39]. However, the direct interaction
444 between PDE1A and STAT3 could not be observed in NSCLC cells. Thus, we
445 next explored the mechanism by which PDE1A promotes the STAT3 signaling
446 pathway. In our study, we demonstrated that PDE1A interacted with YTHDF2
447 and participated in NSCLC progression, and our data first verified the
448 interaction between YTHDF2 and PDE1A in NSCLC cells. Meanwhile,
449 YTHDF2 might act as an m6A RNA “reader” by interacting with PDE1A, but
450 the mechanism might need further investigation. YTHDF2 destabilizes
451 mRNAs via degrading target transcripts, but it also stabilizes important
452 oncogenic drivers, such as *MYC* and *VEGFA* transcripts, in an m6A-
453 dependent manner [40]. We demonstrated that YTHDF2 destabilized SOCS2
454 mRNA and stabilized MET and NRF2 mRNA via interacting with PDE1A, but
455 the mechanism by which YTHDF2 sorts mRNA might need further
456 investigation.

457 Treatment with cisplatin frequently develops chemoresistance leading to
458 therapeutic failure, and the exploitation of chemosensitization strategies have

459 significant clinical implications [41]. In this study, we demonstrated that
460 PDE1A positively regulated the expression of MET and NRF2 in NSCLC cells,
461 and the expression of PDE1A was closely correlated with the anti-NSCLC
462 activity of cisplatin. Our findings are the first to indicate that the expression of
463 PDEs might be involved in NSCLC resistance to cisplatin treatment.
464 Vinpocetine has been clinically used to treat stroke, senile dementia, and
465 memory disturbances; no significant side effects or toxicity of vinpocetine
466 have been reported at therapeutic doses, and it is safe for long-term use [42].
467 Vinpocetine is also regarded as a PDE1 inhibitor and increases the levels of
468 cAMP and cGMP [43]. This study first revealed that vinpocetine sensitized
469 cells to cisplatin treatment via regulating MET and NRF2. Thus, vinpocetine
470 plus cisplatin might be a novel therapeutic regimen for treating NSCLC
471 patients with cisplatin resistance. Our finding was supported by the
472 observations that cAMP signaling increases histone deacetylase 8 expression
473 and augments cisplatin-induced apoptosis [44].
474 Collectively, the results of this study suggest that PDE1A promotes metastasis
475 and cisplatin resistance in NSCLC cells. Furthermore, PDE1A overexpression
476 is correlated with angiogenesis and poor outcomes of NSCLC patients. In
477 addition, PDE1A interacts with YTHDF2 and regulates the JAK/STAT3
478 signaling pathway via degrading SOCS2 mRNA. Meanwhile, PDE1A
479 regulates cisplatin resistance via stabilizing MET and NRF2. Therefore, this
480 study reveals the effect and mechanism of PDE1A in promoting HCC

481 metastasis and cisplatin resistance, this work not only uncovers a novel
482 PDE1A/YTHDF2/STAT3 signaling pathway in NSCLC progression but also
483 provides novel therapeutic strategies to treat NSCLC patients with metastasis
484 or cisplatin resistance.

485 **Acknowledgements**

486 This study was funded by Huadong Medicine Joint Funds of the Zhejiang
487 Provincial Natural Science Foundation of China (LHDMY22H160001), Natural
488 Science Foundation of Ningbo City (2022J206), National Natural Science
489 Foundation of China (82273352), Public-service Technology Research Plan of
490 Zhejiang Province (LGF21H310002), Zhejiang Provincial Natural Science
491 Foundation (LY21H160017).

492 **Authors' contributions**

493 Chong Zhang: Conception and design of the work, drafting the work, writing-
494 original draft, writing-review and editing; Yangling Li: Conception and design
495 of the work, supervision, funding acquisition; Zuoyan Zhang: acquisition,
496 analysis, or interpretation of data for the work; Yuchen Wu: acquisition,
497 analysis, or interpretation of data for the work; Jing Cheng: acquisition,
498 analysis, or interpretation of data for the work; Kaizhi Luo: acquisition,
499 analysis, or interpretation of data for the work; Zhidi Li: acquisition, analysis,
500 or interpretation of data for the work; Manman Zhang: acquisition, analysis, or
501 interpretation of data for the work; Jian Wang: funding acquisition. All authors
502 have approved the final article.

503 **Conflict of Interest**

504 The authors have declared that no competing interest exists.

505 **Availability of data and material**

506 The data presented in the study are included in the article and additional

507 material.

508 **Ethics approval and consent to participate**

509 The experiments were performed in compliance with the National Institutes of

510 Health Guide for the Care and Use of Laboratory Animals.

511 **Consent for publication**

512 Not applicable.

513

514 **Reference**

515 1. A.A. Thai, B.J. Solomon, L.V. Sequist, J.F. Gainor, R.S. Heist, Lung
516 cancer, Lancet. 398 (10299) (2021) 535-554. doi.org/10.1016/S0140-
517 6736(21)00312-3.

518 2. Y. Alduais, H. Zhang, F. Fan, J. Chen, B. Chen, Non-small cell lung
519 cancer (NSCLC): A review of risk factors, diagnosis, and treatment,
520 Medicine (Baltimore). 102 (8) (2023) e32899.
521 doi.org/10.1097/MD.0000000000032899.

522 3. H.W. Xia, Z.Q. Zhang, J. Yuan, Q.L. Niu, Human RECQL5 promotes
523 metastasis and resistance to cisplatin in non-small cell lung cancer, Life
524 Sci. 265 (2021) 118768. doi.org/10.1016/j.lfs.2020.118768.

525 4. H. Chen, L. Wang, J. Liu, Z. Wan, L. Zhou, H. Liao, R. Wan, LncRNA
526 ITGB2-AS1 promotes cisplatin resistance of non-small cell lung cancer
527 by inhibiting ferroptosis via activating the FOSL2/NAMPT axis, Cancer
528 Biol Ther. 24 (1) (2023) 2223377.
529 doi.org/10.1080/15384047.2023.2223377.

530 5. N. Sarin, F. Engel, G.V. Kalayda, M. Mannewitz, J. Cinatl, Jr., F.
531 Rothweiler, M. Michaelis, H. Saafan, C.A. Ritter, U. Jaehde, R.
532 Frotschl, Cisplatin resistance in non-small cell lung cancer cells is
533 associated with an abrogation of cisplatin-induced G2/M cell cycle
534 arrest, PLoS One. 12 (7) (2017) e0181081.
535 doi.org/10.1371/journal.pone.0181081.

536 6. S. Delhaye, B. Bardoni, Role of phosphodiesterases in the
537 pathophysiology of neurodevelopmental disorders, Mol Psychiatry. 26
538 (9) (2021) 4570-4582. doi.org/10.1038/s41380-020-00997-9.
539 7. T. Peng, J. Gong, Y. Jin, Y. Zhou, R. Tong, X. Wei, L. Bai, J. Shi,
540 Inhibitors of phosphodiesterase as cancer therapeutics, Eur J Med
541 Chem. 150 (2018) 742-756. doi.org/10.1016/j.ejmech.2018.03.046.
542 8. G.S. Baillie, G.S. Tejeda, M.P. Kelly, Therapeutic targeting of 3',5'-cyclic
543 nucleotide phosphodiesterases: inhibition and beyond, Nat Rev Drug
544 Discov. 18 (10) (2019) 770-796. doi.org/10.1038/s41573-019-0033-4.
545 9. S. Hsien Lai, G. Zervoudakis, J. Chou, M.E. Gurney, K.M. Quesnelle,
546 PDE4 subtypes in cancer, Oncogene. 39 (19) (2020) 3791-3802.
547 doi.org/10.1038/s41388-020-1258-8.
548 10. W. Huang, J. Sundquist, K. Sundquist, J. Ji, Phosphodiesterase-5
549 inhibitors use and risk for mortality and metastases among male
550 patients with colorectal cancer, Nat Commun. 11 (1) (2020) 3191.
551 doi.org/10.1038/s41467-020-17028-4.
552 11. A. Samidurai, L. Xi, A. Das, A.N. Iness, N.G. Vigneshwar, P.L. Li, D.K.
553 Singla, S. Muniyan, S.K. Batra, R.C. Kukreja, Role of
554 phosphodiesterase 1 in the pathophysiology of diseases and potential
555 therapeutic opportunities, Pharmacol Ther. 226 (2021) 107858.
556 doi.org/10.1016/j.pharmthera.2021.107858.
557 12. R. Liu, J. Miao, Y. Jia, G. Kong, F. Hong, F. Li, M. Zhai, R. Zhang, J.

558 Liu, X. Xu, T. Wang, H. Liu, J. Hu, Y. Yang, A. He, N6-methyladenosine
559 reader YTHDF2 promotes multiple myeloma cell proliferation through
560 EGR1/p21(cip1/waf1)/CDK2-Cyclin E1 axis-mediated cell cycle
561 transition, Oncogene. 42 (20) (2023) 1607-1619.
562 doi.org/10.1038/s41388-023-02675-w.
563 13. X. Chen, X. Zhou, X. Wang, m(6)A binding protein YTHDF2 in cancer,
564 Exp Hematol Oncol. 11 (1) (2022) 21. doi.org/10.1186/s40164-022-
565 00269-y.
566 14. Y. Li, H. Sheng, F. Ma, Q. Wu, J. Huang, Q. Chen, L. Sheng, X. Zhu, X.
567 Zhu, M. Xu, RNA m(6)A reader YTHDF2 facilitates lung
568 adenocarcinoma cell proliferation and metastasis by targeting the
569 AXIN1/Wnt/beta-catenin signaling, Cell Death Dis. 12 (5) (2021) 479.
570 doi.org/10.1038/s41419-021-03763-z.
571 15. S. Ma, B. Sun, S. Duan, J. Han, T. Barr, J. Zhang, M.B. Bissonnette, M.
572 Kortylewski, C. He, J. Chen, M.A. Caligiuri, J. Yu, YTHDF2
573 orchestrates tumor-associated macrophage reprogramming and
574 controls antitumor immunity through CD8(+) T cells, Nat Immunol. 24
575 (2) (2023) 255-266. doi.org/10.1038/s41590-022-01398-6.
576 16. X. Hu, Z.Y. Zhang, L.W. Wu, L.H. Zeng, H. Chen, H.J. Zhu, J.K. Zhang,
577 J. Shao, C. Zhang, Y.L. Li, N.M. Lin, A natural anthraquinone derivative
578 shikonin synergizes with AZD9291 against wtEGFR NSCLC cells
579 through reactive oxygen species-mediated endoplasmic reticulum

580 stress, Phytomedicine. 68 (2020) 153189.
581 doi.org/10.1016/j.phymed.2020.153189.
582 17. M. Uhlen, L. Fagerberg, B.M. Hallstrom, C. Lindskog, P. Oksvold, A.
583 Mardinoglu, A. Sivertsson, C. Kampf, E. Sjostedt, A. Asplund, I. Olsson,
584 K. Edlund, E. Lundberg, S. Navani, C.A. Szigyarto, J. Odeberg, D.
585 Djureinovic, J.O. Takanen, S. Hober, T. Alm, P.H. Edqvist, H. Berling, H.
586 Tegel, J. Mulder, J. Rockberg, P. Nilsson, J.M. Schwenk, M. Hamsten,
587 K. von Feilitzen, M. Forsberg, L. Persson, F. Johansson, M. Zwahlen,
588 G. von Heijne, J. Nielsen, F. Ponten, Proteomics. Tissue-based map of
589 the human proteome, Science. 347 (6220) (2015) 1260419.
590 doi.org/10.1126/science.1260419.
591 18. M. Uhlen, C. Zhang, S. Lee, E. Sjostedt, L. Fagerberg, G. Bidkhori, R.
592 Benfeitas, M. Arif, Z. Liu, F. Edfors, K. Sanli, K. von Feilitzen, P.
593 Oksvold, E. Lundberg, S. Hober, P. Nilsson, J. Mattsson, J.M.
594 Schwenk, H. Brunnstrom, B. Glimelius, T. Sjoblom, P.H. Edqvist, D.
595 Djureinovic, P. Micke, C. Lindskog, A. Mardinoglu, F. Ponten, A
596 pathology atlas of the human cancer transcriptome, Science. 357
597 (6352) (2017) doi.org/10.1126/science.aan2507.
598 19. R. Aguirre-Gamboa, H. Gomez-Rueda, E. Martinez-Ledesma, A.
599 Martinez-Torteya, R. Chacolla-Huaringa, A. Rodriguez-Barrientos, J.G.
600 Tamez-Pena, V. Trevino, SurvExpress: an online biomarker validation
601 tool and database for cancer gene expression data using survival

602 analysis, PLoS One. 8 (9) (2013) e74250.
603 doi.org/10.1371/journal.pone.0074250.
604 20. D. Chitale, Y. Gong, B.S. Taylor, S. Broderick, C. Brennan, R. Somwar,
605 B. Golas, L. Wang, N. Motoi, J. Szoke, J.M. Reinersman, J. Major, C.
606 Sander, V.E. Seshan, M.F. Zakowski, V. Rusch, W. Pao, W. Gerald, M.
607 Ladanyi, An integrated genomic analysis of lung cancer reveals loss of
608 DUSP4 in EGFR-mutant tumors, Oncogene. 28 (31) (2009) 2773-2783.
609 doi.org/10.1038/onc.2009.135.
610 21. S. Rousseaux, A. Debernardi, B. Jacquiau, A.L. Vitte, A. Vesin, H.
611 Nagy-Mignotte, D. Moro-Sibilot, P.Y. Brichon, S. Lantuejoul, P. Hainaut,
612 J. Laffaire, A. de Reynies, D.G. Beer, J.F. Timsit, C. Brambilla, E.
613 Brambilla, S. Khochbin, Ectopic activation of germline and placental
614 genes identifies aggressive metastasis-prone lung cancers, Sci Transl
615 Med. 5 (186) (2013) 186ra166. doi.org/10.1126/scitranslmed.3005723.
616 22. C.P. Goswami, H. Nakshatri, PROGgeneV2: enhancements on the
617 existing database, BMC Cancer. 14 (2014) 970. doi.org/10.1186/1471-
618 2407-14-970.
619 23. S.V. Vasaikar, P. Straub, J. Wang, B. Zhang, LinkedOmics: analyzing
620 multi-omics data within and across 32 cancer types, Nucleic Acids Res.
621 46 (D1) (2018) D956-D963. doi.org/10.1093/nar/gkx1090.
622 24. A. Onn, R.S. Herbst, Angiogenesis, metastasis, and lung cancer. An
623 overview, Methods Mol Med. 74 (2003) 329-348. doi.org/10.1385/1-

624 59259-323-2:329.
625 25. D.S. Chandrashekar, B. Bashel, S.A.H. Balasubramanya, C.J.
626 Creighton, I. Ponce-Rodriguez, B. Chakravarthi, S. Varambally,
627 UALCAN: A Portal for Facilitating Tumor Subgroup Gene Expression
628 and Survival Analyses, Neoplasia. 19 (8) (2017) 649-658.
629 doi.org/10.1016/j.neo.2017.05.002.
630 26. H. Shi, X. Wang, Z. Lu, B.S. Zhao, H. Ma, P.J. Hsu, C. Liu, C. He,
631 YTHDF3 facilitates translation and decay of N(6)-methyladenosine-
632 modified RNA, Cell Res. 27 (3) (2017) 315-328.
633 doi.org/10.1038/cr.2017.15.
634 27. A. Bartha, B. Gyorffy, TNMplot.com: A Web Tool for the Comparison of
635 Gene Expression in Normal, Tumor and Metastatic Tissues, Int J Mol
636 Sci. 22 (5) (2021) doi.org/10.3390/ijms22052622.
637 28. E. Cerami, J. Gao, U. Dogrusoz, B.E. Gross, S.O. Sumer, B.A. Aksoy,
638 A. Jacobsen, C.J. Byrne, M.L. Heuer, E. Larsson, Y. Antipin, B. Reva,
639 A.P. Goldberg, C. Sander, N. Schultz, The cBio cancer genomics
640 portal: an open platform for exploring multidimensional cancer
641 genomics data, Cancer Discov. 2 (5) (2012) 401-404.
642 doi.org/10.1158/2159-8290.CD-12-0095.
643 29. J. Gao, B.A. Aksoy, U. Dogrusoz, G. Dresdner, B. Gross, S.O. Sumer,
644 Y. Sun, A. Jacobsen, R. Sinha, E. Larsson, E. Cerami, C. Sander, N.
645 Schultz, Integrative analysis of complex cancer genomics and clinical

646 profiles using the cBioPortal, Sci Signal. 6 (269) (2013) pl1.
647 doi.org/10.1126/scisignal.2004088.
648 30. U.K. Muppirala, V.G. Honavar, D. Dobbs, Predicting RNA-protein
649 interactions using only sequence information, BMC Bioinformatics. 12
650 (2011) 489. doi.org/10.1186/1471-2105-12-489.
651 31. B. Sen, S. Peng, D.M. Woods, I. Wistuba, D. Bell, A.K. El-Naggar, S.Y.
652 Lai, F.M. Johnson, STAT5A-mediated SOCS2 expression regulates
653 Jak2 and STAT3 activity following c-Src inhibition in head and neck
654 squamous carcinoma, Clin Cancer Res. 18 (1) (2012) 127-139.
655 doi.org/10.1158/1078-0432.CCR-11-1889.
656 32. G.E. Wood, H. Hockings, D.M. Hilton, S. Kermorgant, The role of MET
657 in chemotherapy resistance, Oncogene. 40 (11) (2021) 1927-1941.
658 doi.org/10.1038/s41388-020-01577-5.
659 33. S. Mirzaei, A.T. Mohammadi, M.H. Gholami, F. Hashemi, A. Zarrabi, A.
660 Zabolian, K. Hushmandi, P. Makvandi, M. Samec, A. Liskova, P.
661 Kubatka, N. Nabavi, A.R. Aref, M. Ashrafizadeh, H. Khan, M. Najafi,
662 Nrf2 signaling pathway in cisplatin chemotherapy: Potential
663 involvement in organ protection and chemoresistance, Pharmacol Res.
664 167 (2021) 105575. doi.org/10.1016/j.phrs.2021.105575.
665 34. T. Zhu, X. Bao, M. Chen, R. Lin, J. Zhuyan, T. Zhen, K. Xing, W. Zhou,
666 S. Zhu, Mechanisms and Future of Non-Small Cell Lung Cancer
667 Metastasis, Front Oncol. 10 (2020) 585284.

668 doi.org/10.3389/fonc.2020.585284.
669 35. S. Chen, C. Yan, An update of cyclic nucleotide phosphodiesterase as
670 a target for cardiac diseases, Expert Opin Drug Discov. 16 (2) (2021)
671 183-196. doi.org/10.1080/17460441.2020.1821643.
672 36. R. Kakkar, R.V. Raju, R.K. Sharma, Calmodulin-dependent cyclic
673 nucleotide phosphodiesterase (PDE1), Cell Mol Life Sci. 55 (8-9)
674 (1999) 1164-1186. doi.org/10.1007/s000180050364.
675 37. Q.F. Han, W.J. Li, K.S. Hu, J. Gao, W.L. Zhai, J.H. Yang, S.J. Zhang,
676 Exosome biogenesis: machinery, regulation, and therapeutic
677 implications in cancer, Mol Cancer. 21 (1) (2022) 207.
678 doi.org/10.1186/s12943-022-01671-0.
679 38. S.W. Messenger, S.S. Woo, Z. Sun, T.F.J. Martin, A Ca(2+)-stimulated
680 exosome release pathway in cancer cells is regulated by Munc13-4, J
681 Cell Biol. 217 (8) (2018) 2877-2890. doi.org/10.1083/jcb.201710132.
682 39. J. Mohrherr, I.Z. Uras, H.P. Moll, E. Casanova, STAT3: Versatile
683 Functions in Non-Small Cell Lung Cancer, Cancers (Basel). 12 (5)
684 (2020) doi.org/10.3390/cancers12051107.
685 40. D. Dixit, B.C. Prager, R.C. Gimple, H.X. Poh, Y. Wang, Q. Wu, Z. Qiu,
686 R.L. Kidwell, L.J.Y. Kim, Q. Xie, K. Vitting-Seerup, S. Bhargava, Z.
687 Dong, L. Jiang, Z. Zhu, P. Hamerlik, S.R. Jaffrey, J.C. Zhao, X. Wang,
688 J.N. Rich, The RNA m6A Reader YTHDF2 Maintains Oncogene
689 Expression and Is a Targetable Dependency in Glioblastoma Stem

690 Cells, Cancer Discov. 11 (2) (2021) 480-499. doi.org/10.1158/2159-
691 8290.CD-20-0331.
692 41. L. Galluzzi, L. Senovilla, I. Vitale, J. Michels, I. Martins, O. Kepp, M.
693 Castedo, G. Kroemer, Molecular mechanisms of cisplatin resistance,
694 Oncogene. 31 (15) (2012) 1869-1883. doi.org/10.1038/onc.2011.384.
695 42. Y.S. Zhang, J.D. Li, C. Yan, An update on vinpocetine: New discoveries
696 and clinical implications, Eur J Pharmacol. 819 (2018) 30-34.
697 doi.org/10.1016/j.ejphar.2017.11.041.
698 43. N.J. Kim, J.H. Baek, J. Lee, H. Kim, J.K. Song, K.H. Chun, A PDE1
699 inhibitor reduces adipogenesis in mice via regulation of lipolysis and
700 adipogenic cell signaling, Exp Mol Med. 51 (1) (2019) 1-15.
701 doi.org/10.1038/s12276-018-0198-7.
702 44. J.Y. Park, Y.S. Juhnn, cAMP signaling increases histone deacetylase 8
703 expression via the Epac2-Rap1A-Akt pathway in H1299 lung cancer
704 cells, Exp Mol Med. 49 (2) (2017) e297.
705 doi.org/10.1038/emm.2016.152.
706
707

708 **Figure legends**

709 **Figure 1. High expression of PDE1A predicts a poor prognosis of lung**
710 **cancer patients.** (A) The expression of PDE1A was detected in lung cancer
711 and normal lung tissue. The data were obtained from The Human Protein
712 Atlas (https://www.proteinatlas.org). (B) The expression of PDE1A in HELF,
713 A549, NCI-H1299, and NCI-H460 cells was detected by western blot. (C and
714 D) Box plot analysis of the PDE1A mRNA levels in clinical lung cancer tissue
715 samples. The data were collected from SurvExpress
716 (http://bioinformatica.mty.itesm.mx:8080/Biomatec/SurvivaX.jsp). Gene:
717 PDE1A; Access database Numbers: Chitale Lung (n=185); Censored:
718 Recurrence Months or Survival months. (E) The data was collected from
719 PROGgene V2 Prognostic Database
720 (http://www.progtools.net/gene/index.php). Single user input genes: PDE1A;
721 Cancer type: LUNG; Survival measure: Death; Bifurcate gene expression at:
722 Median; GSE30219-Off-context gene expression in lung cancer identifies a
723 group of metastatic-prone tumors.

724 **Figure 2: PDE1A knockdown suppresses the metastasis of NSCLC cells.**
725 (A-B) NSCLC cells were transfected with control siRNA and PDE1A siRNA for
726 24 h, cells were transferred to Transwell chambers without (A) or with (B) a
727 Matrigel coating on the insert membrane, and the cell migrative and invasive
728 abilities were determined, respectively. (C-D) NSCLC cells were transfected
729 with control siRNA and PDE1A siRNA for 24 h, and the wound healing assay

730 was established in NSCLC cells. (E) NSCLC cells were transfected with
731 control siRNA and PDE1A siRNA for 48 h, and the expression of indicated
732 proteins were detected. (F-G) NSCLC cells were treated with DMSO or
733 vinpocetine (5, 10, 20 μM) for 24 h, and the migrative ability of treated NSCLC
734 cells was determined using Transwell assay for 24 h. (H) NSCLC cells were
735 treated with DMSO or vinpocetine (5, 10, 20 μM) for 24 h, and the expression
736 of indicated proteins was determined. (I) The pulmonary metastatic nodules
737 were stained using H&E staining and counted in nude mice harboring NCI-
738 H1299 cells transfected with PDE1A shRNA and control shRNA.

739 **Figure 3: PDE1A promotes the metastasis and EMT of NSCLC cells.** (A-
740 B) NSCLC cells were transfected with PDE1A plasmid and empty vector for
741 24 h, cells were transferred to Transwell chambers without (A) or with (B) a
742 Matrigel coating on the insert membrane, and the cell migrative and invasive
743 abilities were determined, respectively. (C) NSCLC cells were transfected with
744 PDE1A plasmid and empty vector for 24 h, and the wound-healing assay was
745 established in NSCLC cells. (D) NSCLC cells were transfected with PDE1A
746 plasmid and empty vector for 48 h, and the expression of indicated proteins
747 were detected. (E) The highly invasive NSCLC cells were separated using
748 transwell chamber assay, and P3 cells were obtained from P0 cells after three
749 generations. (F-G) The protein (F) and mRNA (G) levels of indicated genes
750 were determined in P3 and P0 NSCLC cells. (H) The pulmonary metastatic
751 nodules were stained using H&E and Bouin's solution and counted in nude

752 mice harboring NCI-H1299 cells transfected with PDE1A plasmid and empty
753 vector.

754 **Figure 4: NSCLC cells overexpressing PDE1A promote angiogenesis in**
755 **the TME.** (A) Data were collected from LinkedOmics. (B-D) NSCLC cells were
756 transfected with empty vector / PDE1A overexpressing plasmid or control
757 siRNA / siPDE1A for 48 h, and then NSCLC cells were placed on the upper
758 panel of transwell with 0.4 μm insert, HUVECs were placed on the lower panel
759 of transwell, and wound healing assay was performed to determine the
760 migrative abilities of HUVECs. (E) NSCLC cells with PDE1A overexpression
761 were treated with 10 μM GW4869, and wound healing assay was performed
762 to determine the migrative abilities of HUVECs. (F) NSCLC cells were
763 transfected with empty vector or shPDE1A, then cells were transplanted into
764 nude mice via subcutaneous injection, the blood vessels were counted after
765 60 days.

766 **Figure 5: PDE1A promotes the metastasis of NSCLC cells via STAT3**
767 **signaling pathway.** (A) A Venn diagram was generated using LinkedOmics,
768 ORA was performed to analysis the molecular pathway regulated by PDE1A
769 in NSCLC. Sample cohort: TCGA_NSCLC; Institute: UNC; Data type:
770 RNAseq; Platform: HiSeq RNA; Attribute: PDE1A; Statistical methods:
771 Spearman Correlation test; Patients: 515; Tools: ORA; Gene Ontology
772 analysis: Wikipathway and Panther Pathway; Select Rank Criteria: FDR;
773 Select Sign: Positively correlated; Significance Level: 0.05; TOP40 was

774 selected to generate Venn diagram. (B) GSEA was performed to analyze the
775 biological process of PDE1A in NSCLC. (C) NSCLC cells were transfected
776 with PDE1A plasmid and empty vector for 48 h, and the expression of
777 indicated proteins were detected. (D) NSCLC cells were transfected with
778 control siRNA and PDE1A siRNA for 48 h, and the expression of indicated
779 proteins were detected. (E) NSCLC cells were treated with DMSO or
780 vinpocetine (5, 10, 20 μM) for 24 h, and the expression of indicated proteins
781 was determined. (F) NSCLC cells overexpressing PDE1A were transfected
782 with control siRNA and STAT3 siRNA for 48 h, the migrative abilities of
783 NSCLC cells were determined by Transwell assay. (G) NSCLC cells
784 overexpressing PDE1A were treated with STAT3 inhibitor SH-4-54 (5 μM) for
785 24 h, the migrative abilities of NSCLC cells were determined by Transwell
786 assay. (H) NSCLC cells overexpressing PDE1A were transfected with control
787 siRNA and STAT3 siRNA for 48 h, and the expression of indicated protein was
788 detected by western blot. (I) NSCLC cells overexpressing PDE1A were
789 treated with STAT3 inhibitor SH-4-54 (5 μM) for 24 h, and the expression of
790 indicated protein was detected by western blot. (J) The interaction between
791 PDE1A and STAT3 was determined by immunoprecipitation. (K) NCI-H1299
792 cells were transfected with empty vector and PDE1A overexpressing plasmid
793 for 48 h, and the contribution of PDE1A in the cytoplasm and nucleus was
794 determined.

795 **Figure 6: PDE1A physically interacts with YTHDF2 and promotes the**

796 **metastasis of NSCLC cells.** (A) Venn diagram showing the overlap among
797 PDE1A interacting proteins (The data was collected from mass spectrometry
798 analysis in NSCLC cells), STAT3 coexpressed genes (collected from gene
799 correlation using UALCAN), upregulated proteins in NSCLC compared with
800 normal tissues (analyzed by UALCAN based on CPTAC database), and
801 upregulated genes in NSCLC compared with normal tissues (analyzed by
802 UALCAN based on TCGA database). (B) GO enrichment analysis of PDE1A
803 interacting genes. (C) Immunoprecipitation followed by silver staining was
804 performed to identify protein and protein interaction using A549 cell lysate with
805 the anti-PDE1A antibody. (D) Immunoprecipitation was used to confirm protein
806 and protein interaction in NCI-H1299 cells. (E) NSCLC cells overexpressing
807 PDE1A were transfected with control siRNA and YTHDF2 siRNA for 48 h, the
808 migrative abilities of NSCLC cells were determined by Transwell assay. (F)
809 NSCLC cells overexpressing PDE1A were transfected with control siRNA and
810 YTHDF2 siRNA for 48 h, and the expression of indicated protein was detected
811 by western blot. (G) The Pearson correlation coefficient between the
812 expression of YTHDF2 and STAT3 was identified using UALCAN.

813 **Figure 7: PDE1A interacts with YTHDF2 to regulate SOCS2/STAT3**
814 **signaling pathway.** (A) YTHDF2-RNA complexes were identified by LC-
815 MS/MS and collected from reference; YTHDF2 corelated genes were
816 collected from TNMplot (https://tnmplot.com/analysis/), Gene: YTHDF2, Gene
817 vs. all genes correlation: Genechip data, Tissue: Lung; STAT3 corelated

818 genes were collected from cBioPortal (http://www.cbioportal.org/), Lung
819 cancer (SMC, cancer research 2016); n=22; Gene: STAT3. The interaction
820 between YTHDF2 protein and the mRNA of 33 overlapping genes were
821 predicted by RNA-Protein Interaction Prediction
822 (http://pridb.gdcb.iastate.edu/RPISeq/index.html), and the values of RF
823 classifier and SVM classifier above 0.5 were considered positive. (B) The
824 interactions between protein and mRNAs were verified by RIP experiments.
825 (C) NSCLC cells were transfected with control siRNA and siPDE1A for 48 h,
826 and the stability of mRNA was determined by qRT-PCR. (D) NSCLC cells
827 were transfected with control siRNA and siPDE1A for 48 h, and the
828 expression of SOCS2 mRNA was determined by qRT-PCR.

829 **Figure 8: PDE1A suppression enhances anti-NSCLC activity of cisplatin**
830 **via regulating MET and NRF2 expression.** (A) NSCLC cells were
831 transfected with control siRNA or siPDE1A for 48 h, and the expression of
832 indicated proteins were determined. (B) NSCLC cells were transfected with
833 empty vector or PDE1A overexpressing plasmid for 48 h, and the expression
834 of indicated proteins were determined. (C) NSCLC cells were treated with
835 vinpocetine for 24 h, and the expression of indicated proteins were
836 determined. (D) NSCLC cells were transfected with control siRNA or siPDE1A
837 for 24 h, and then cells were treated with cisplatin for 72 h, SRB assay was
838 performed to evaluate cell proliferation. (E) NSCLC cells were transfected with
839 empty vector or PDE1A overexpressing plasmid for 24 h, and then cells were

840 treated with cisplatin for 72 h, SRB assay was performed to evaluate cell
841 proliferation. (F) NSCLC cells were treated with vinpocetine and/or cisplatin
842 for 72 h, and SRB assay was performed to evaluate cell proliferation. (G)
843 NSCLC cells were treated with vinpocetine and/or cisplatin for 48 h, and the
844 expression of indicate proteins were detected. (H) NSCLC cells were
845 transfected with control siRNA or siPDE1A for 48 h, and the mRNA level of
846 indicated proteins were determined. (I) NSCLC cells overexpressing PDE1A
847 were transfected with control siRNA and YTHDF2 siRNA for 48 h, and the
848 expression of the indicated proteins was detected.

849 **Supplementary information**

850 1. Supplementary file 1: Figure S1. tif

851 The expression of PDE1A in normal lung (A) and lung cancer (B). The data
852 were obtained from The Human Protein Atlas (https://www.proteinatlas.org).

853 2. Supplementary file 2: Figure S2. tif

854 The biological processes related to PDE1A in NSCLC is predicted using the
855 LinkedOmics. Data collected from LinkedOmics
856 (www.linkedomics.org/admin.php) are shown. ORA (A) and GSEA (B) were
857 performed to analyze the biological processes related to PDE1A in NSCLC.
858 Sample cohort: TCGA_NSCLC; Institute: UNC; Data type: RNAseq; Platform:
859 HiSeq RNA; Attribute: PDE1A; Statistical methods: Spearman Correlation
860 test; Patients: 515; Tools: ORA and GSEA; Gene Ontology analysis: biological
861 process. (C) GSEA demonstrated that PDE1A participated in mesenchyme

862 development and the cellular response to VEGF stimulus.

863 3. Supplementary file 3: Figure S3. tif

864 The expression of PDE1A does not affect the proliferation of NSCLC cells. (A-
865 B) NSCLC cells were transfected with PDE1A siRNA or control siRNA (A) and
866 empty vector or PDE1A plasmid (B) for 24 h in 6-well plates, then transferred
867 to 96-well plated for the indicated times, and finally subjected to SRB assay.

868 4. Supplementary file 4: Figure S4.tif

869 PDE1A silence suppresses the metastasis of NSCLC cells. (A) NSCLC cells
870 were transfected with control siRNA, siPDE1A, siPDE1B, and siPDE1C for 24
871 h, and cells were transferred to Transwell chambers without a Matrigel coating
872 on the insert membrane, and the cell migration were determined after 24 h.
873 (B) NSCLC cells were transfected with indicated siRNA for 48 h, and the
874 expression of the indicated proteins were detected. (C) The lungs of nude
875 mice were separated and stained with Bouin's solution and the pulmonary
876 metastatic nodules were counted.

877 5. Supplementary file 5: Figure S5.tif

878 PDE1A promotes the metastasis of NSCLC cells. (A) The migrative abilities of
879 P3 and P0 NSCLC cells were determined. (B) The mRNA levels of indicated
880 genes were determined in P3 and P0 NSCLC cells using qRT-PCR. (C)
881 Before the NSCLC cells were injected into the nude mice, the migrative
882 abilities of NSCLC cells were determined using Transwell assay.

883 6. Supplementary file 6: Figure S6. tif

884 PDE1A promotes the metastatic potential in a cAMP-independent manner. (A)
885 NSCLC cells were transfected with control siRNA and PDE1A siRNA, after 24
886 h cells were collected for Transwell assay, cells were treated with DMSO or 5
887 μM SQ22536 for 24 h, and the migrative abilities of NSCLC cells were
888 determined. (B-C) NSCLC cells were transfected with control siRNA and
889 YTHDF2 siRNA for 48 h, and the knockdown efficiency of YTHDF2 was
890 confirmed by western blot (B) and qRT-PCR (C).

891 7. Supplementary file 7: Figure S7. tif

892 Overexpression of YTHDF2 predicts poor outcomes for lung cancer patients.
893 (A-B) The mRNA and protein levels of PDE1A in NSCLC and normal lung
894 tissues are shown. Data collected from UALCAN was shown. Gene: YTHDF2;
895 TCGA dataset: Lung adenocarcinoma (A); CPTAC dataset: Lung
896 adenocarcinoma (B). (C) The prognostics value of YTHDF2 in NSCLC
897 patients was identified using PROGgeneV2 online tool
898 (www.progtools.net/gene).

899 8. Supplementary file 8: Table S1. xls

900 The siRNA sequence used for knocking down the indicated genes.

901 9. Supplementary file 9: Table S2. xls

902 Primers sequences for detecting the expression of the indicated genes.

903 10. Supplementary file 10: Table S3. xls

904 Identification of PDE1A protein interactions by mass spectrometry.

905 11. Supplementary file 11: Table S4. xls

906 The potential target genes of YTHDF2 in NSCLC cells.

907 12. Supplementary file 12: Table S5. xls

908 The potential target genes of YTHDF2 in NSCLC cells.

909

Figure 1

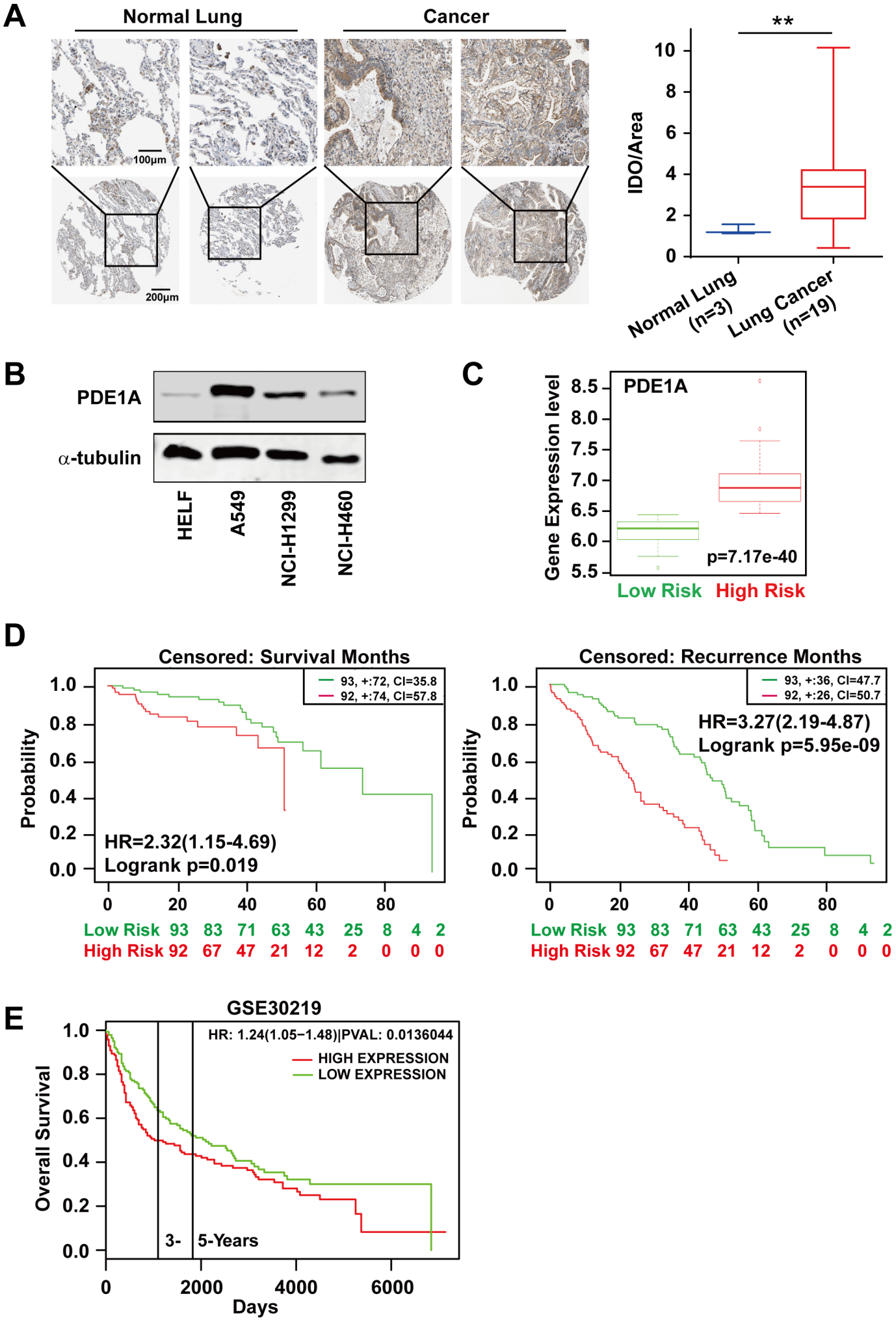
A
Normal Lung
Cancer
100μm
200μm
**
IDO/Area
10
8
6
4
2
0
Normal Lung (n=3)
Lung Cancer (n=19)
B
PDE1A
α-tubulin
HELF
A549
NCI-H1299
NCI-H460
C
PDE1A
Gene Expression level
8.5
8.0
7.5
7.0
6.5
6.0
5.5
p=7.17e-40
Low Risk
High Risk
D
Censored: Survival Months
93, +:72, CI=35.8
92, +:74, CI=57.8
Probability
HR=2.32(1.15-4.69)
Logrank p=0.019
0 20 40 60 80
Low Risk 93 83 71 63 43 25 8 4 2
High Risk 92 67 47 21 12 2 0 0 0
Censored: Recurrence Months
93, +:36, CI=47.7
92, +:26, CI=50.7
HR=3.27(2.19-4.87)
Logrank p=5.95e-09
Low Risk 93 83 71 63 43 25 8 4 2
High Risk 92 67 47 21 12 2 0 0 0
E
GSE30219
HR: 1.24(1.05−1.48)|PVAL: 0.0136044
HIGH EXPRESSION
LOW EXPRESSION
Overall Survival
3- 5-Years
0 2000 4000 6000
Days

Figure 2

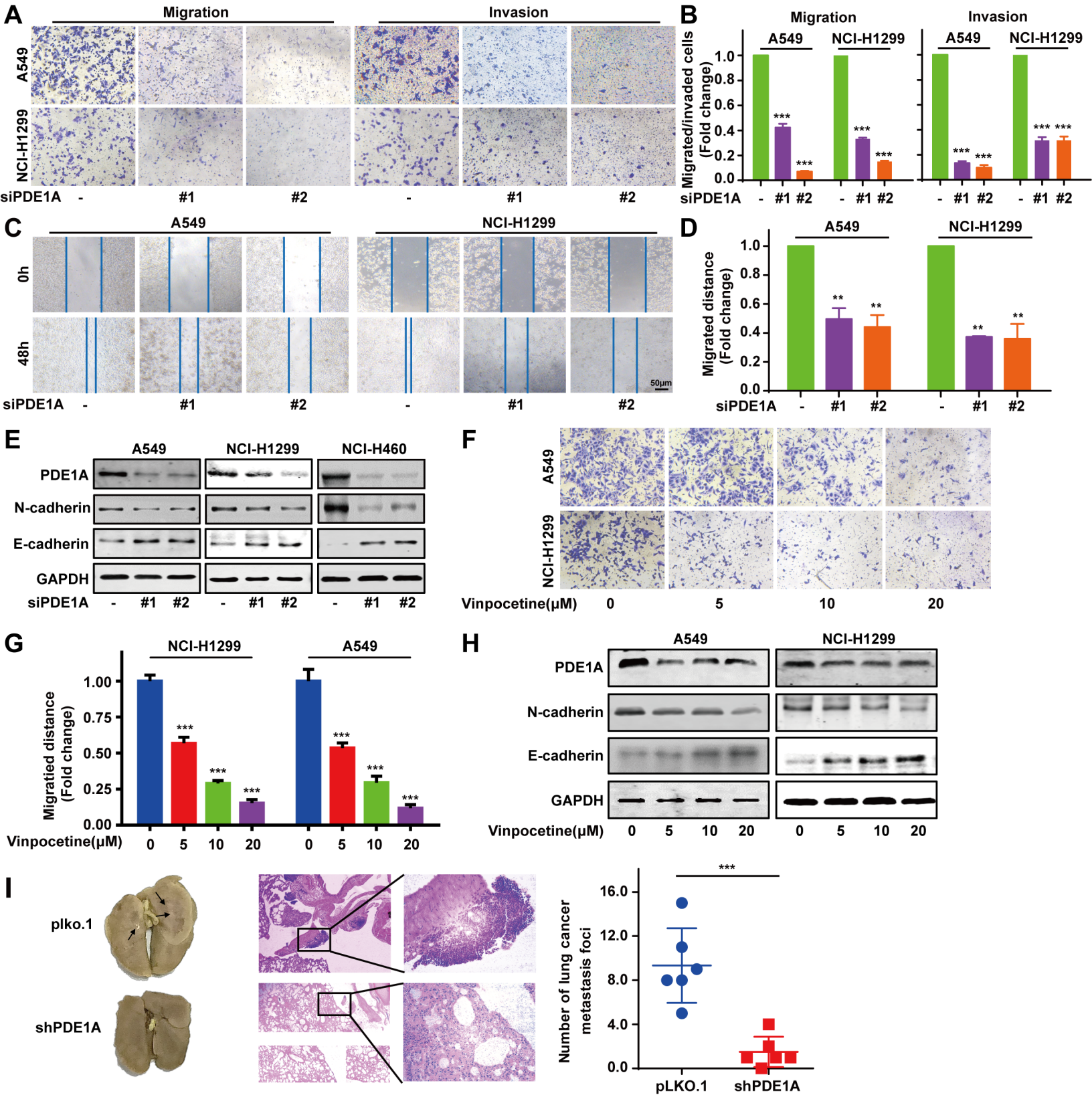
A
Migration
Invasion
A549
NCI-H1299
siPDE1A - #1 #2 - #1 #2
B
Migration
Invasion
A549
NCI-H1299
Migrated/invaded cells (Fold change)
1.0
0.8
0.6
0.4
0.2
0.0
***
siPDE1A - #1 #2 - #1 #2 - #1 #2 - #1 #2
C
A549
NCI-H1299
0h
48h
50μm
siPDE1A - #1 #2 - #1 #2
D
A549
NCI-H1299
Migrated distance (Fold change)
1.0
0.8
0.6
0.4
0.2
0.0
**
siPDE1A - #1 #2 - #1 #2
E
A549
NCI-H1299
NCI-H460
PDE1A
N-cadherin
E-cadherin
GAPDH
siPDE1A - #1 #2 - #1 #2 - #1 #2
F
A549
NCI-H1299
Vinpocetine(μM) 0 5 10 20
G
NCI-H1299
A549
Migratied distance (Fold change)
1.00
0.75
0.50
0.25
0.00
***
Vinpocetine(μM) 0 5 10 20 0 5 10 20
H
A549
NCI-H1299
PDE1A
N-cadherin
E-cadherin
GAPDH
Vinpocetine(μM) 0 5 10 20 0 5 10 20
I
plko.1
shPDE1A
Number of lung cancer metastasis foci
16.0
12.0
8.0
4.0
0.0
***
pLKO.1
shPDE1A

Figure 3

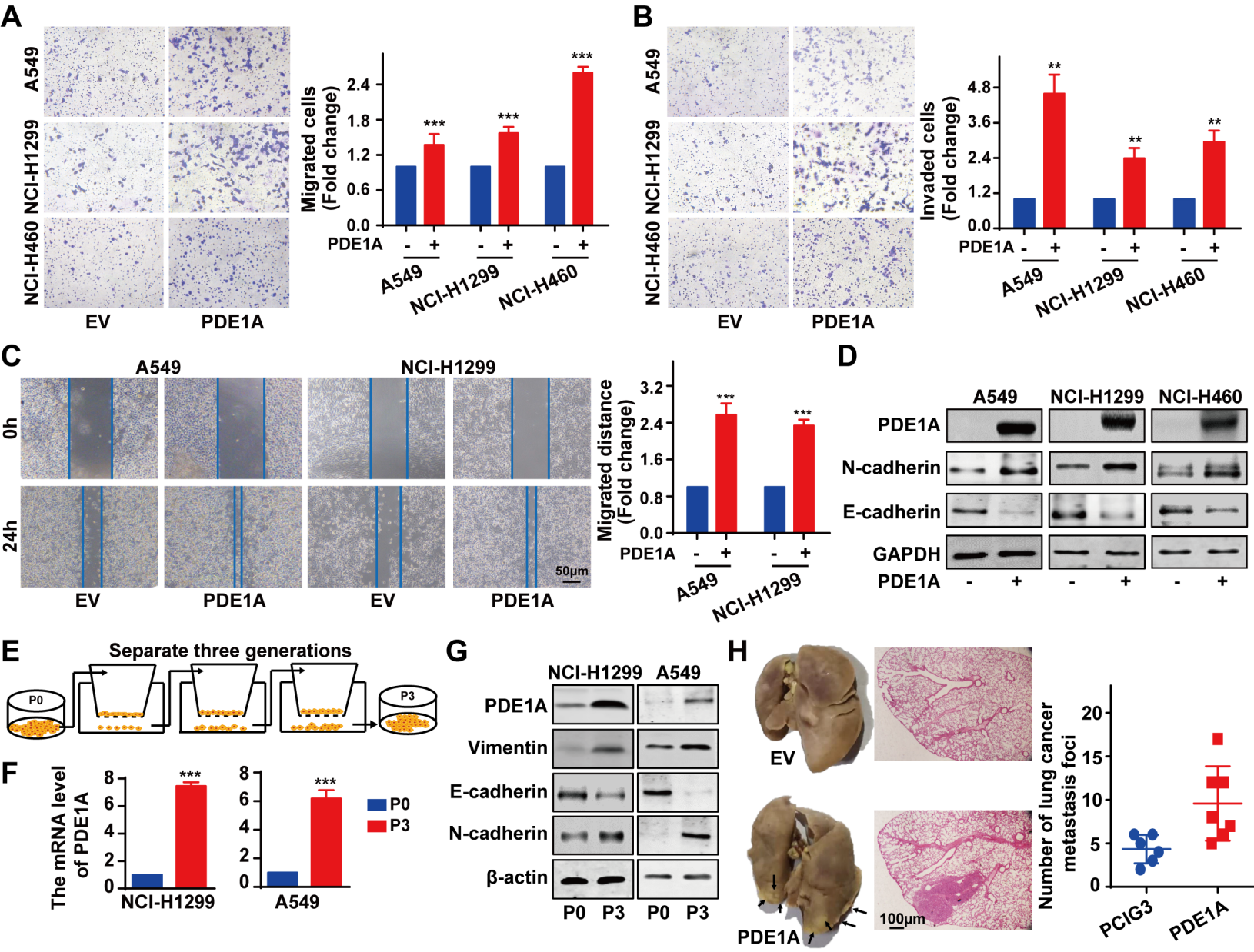
A
A549
NCI-H1299
NCI-H460
EV
PDE1A
Migrated cells (Fold change)
PDE1A
B
Invaded cells (Fold change)
C
0h
24h
50μm
Migrated distance (Fold change)
D
PDE1A
N-cadherin
E-cadherin
GAPDH
E
Separate three generations
P0
P3
F
The mRNA level of PDE1A
G
Vimentin
β-actin
H
100μm
Number of lung cancer metastasis foci
PCIG3

Figure 4

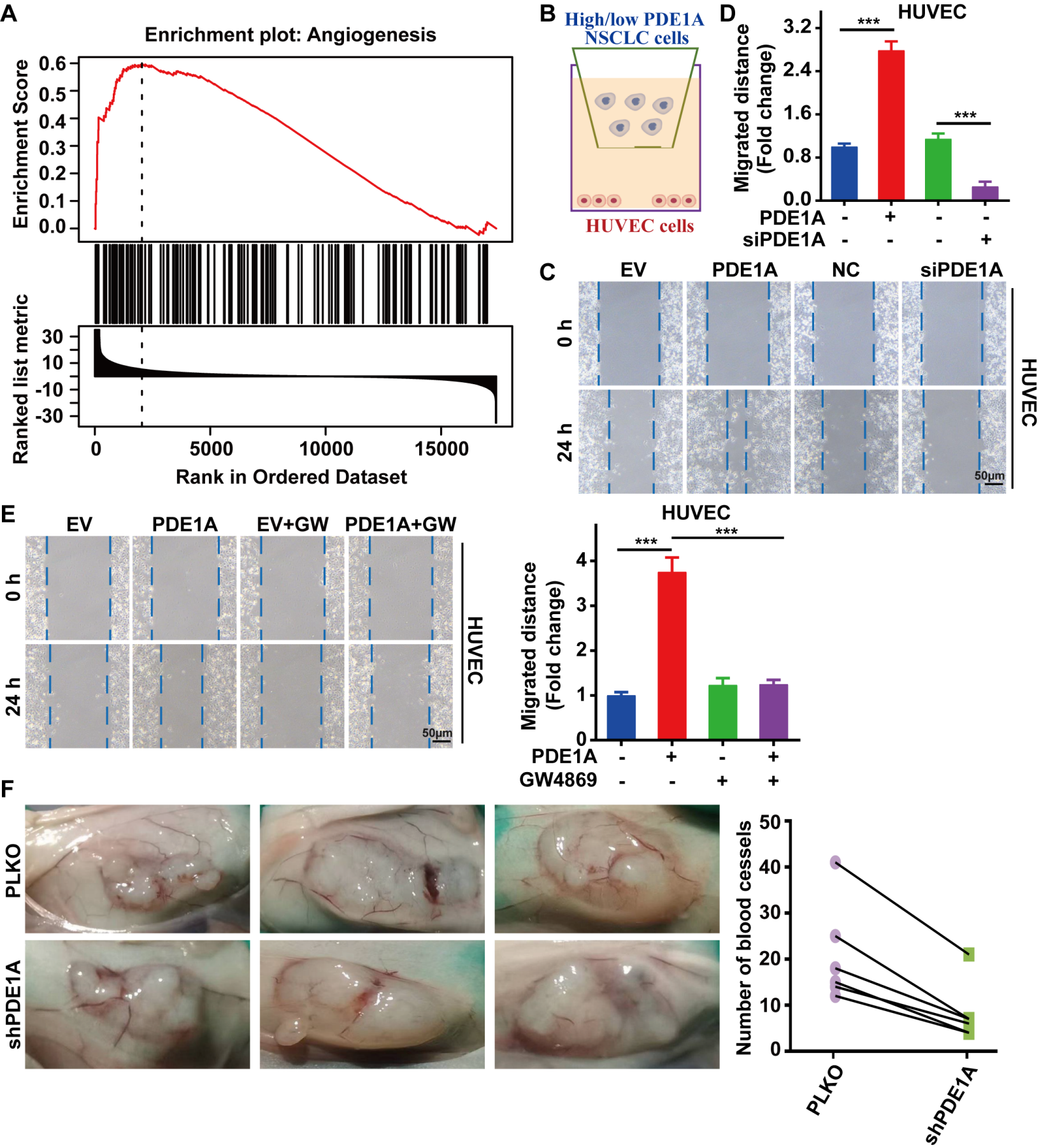
A
Enrichment plot: Angiogenesis
Enrichment Score
0.6
0.5
0.4
0.3
0.2
0.1
0.0
Ranked list metric
30
10
-10
-30
0
5000
10000
15000
Rank in Ordered Dataset
B
High/low PDE1A NSCLC cells
HUVEC cells
D
HUVEC
Migrated distance (Fold change)
3.2
2.4
1.6
0.8
0.0
***
***
PDE1A - + - -
siPDE1A - - - +
C
EV
PDE1A
NC
siPDE1A
0 h
24 h
HUVEC
50μm
E
EV
PDE1A
EV+GW
PDE1A+GW
0 h
24 h
HUVEC
50μm
HUVEC
Migrated distance (Fold change)
4
3
2
1
0
***
***
PDE1A - + - +
GW4869 - - + +
F
PLKO
shPDE1A
Number of blood cessels
50
40
30
20
10
0
PLKO
shPDE1A

Figure 5

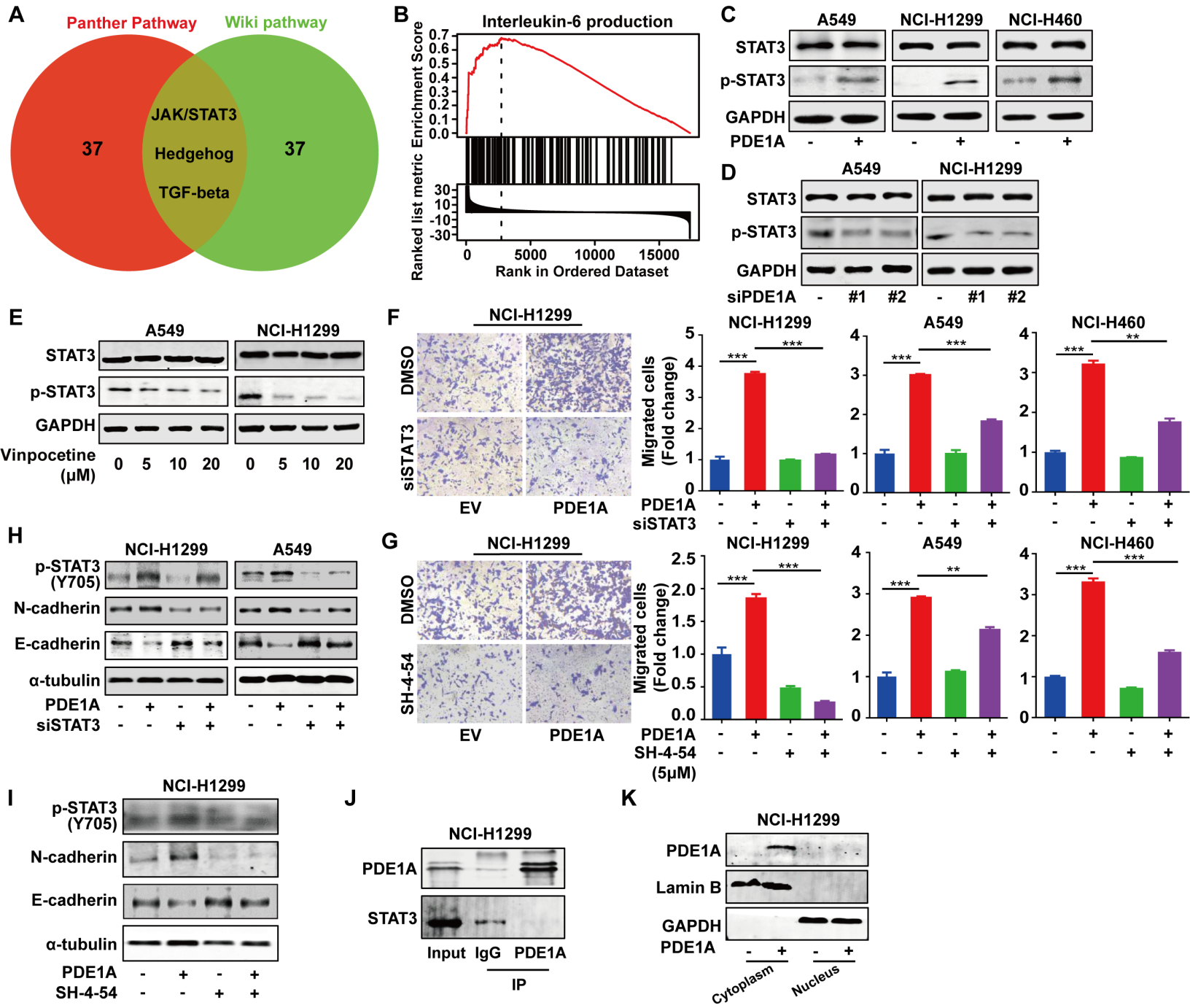
A
Panther Pathway
Wiki pathway
37
JAK/STAT3
Hedgehog
TGF-beta
37
B
Interleukin-6 production
Enrichment Score
Ranked list metric
Rank in Ordered Dataset
C
A549
NCI-H1299
NCI-H460
STAT3
p-STAT3
GAPDH
PDE1A
D
A549
NCI-H1299
STAT3
p-STAT3
GAPDH
siPDE1A
#1
#2
E
A549
NCI-H1299
STAT3
p-STAT3
GAPDH
Vinpocetine (μM)
F
NCI-H1299
DMSO
siSTAT3
EV
PDE1A
Migrated cells (Fold change)
PDE1A
siSTAT3
G
NCI-H1299
DMSO
SH-4-54
EV
PDE1A
Migrated cells (Fold change)
PDE1A
SH-4-54 (5μM)
H
NCI-H1299
A549
p-STAT3 (Y705)
N-cadherin
E-cadherin
α-tubulin
PDE1A
siSTAT3
I
NCI-H1299
p-STAT3 (Y705)
N-cadherin
E-cadherin
α-tubulin
PDE1A
SH-4-54
J
NCI-H1299
PDE1A
STAT3
Input
IgG
PDE1A
IP
K
NCI-H1299
PDE1A
Lamin B
GAPDH
PDE1A
Cytoplasm
Nucleus

Figure 6

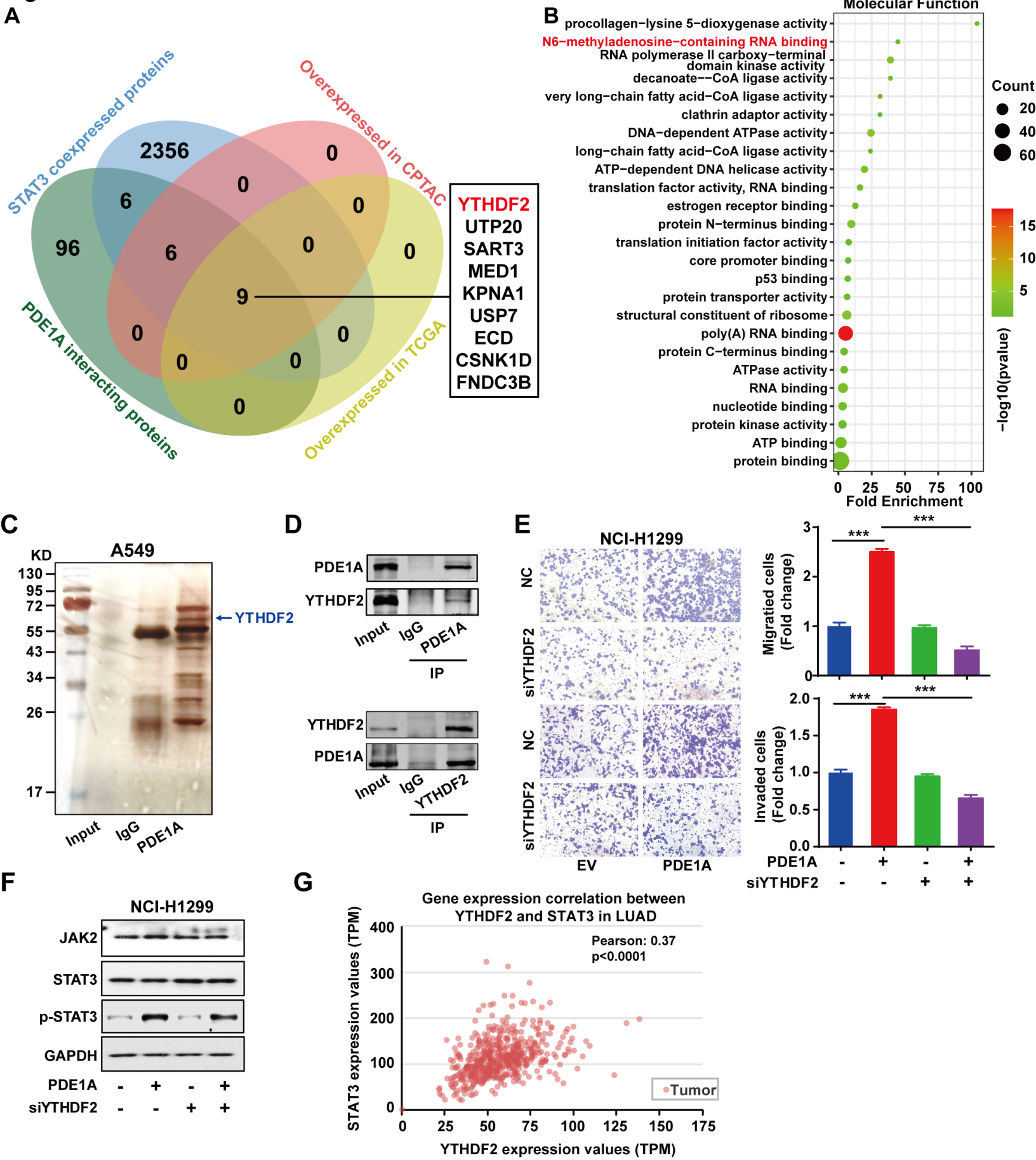
A
STAT3 coexpressed proteins
Overexpressed in CPTAC
PDE1A interacting proteins
Overexpressed in TCGA
2356
96
6
6
0
0
0
0
0
0
0
0
0
0
9
YTHDF2
UTP20
SART3
MED1
KPNA1
USP7
ECD
CSNK1D
FNDC3B
B
Molecular Function
procollagen-lysine 5-dioxygenase activity
N6-methyladenosine-containing RNA binding
RNA polymerase II carboxy-terminal domain kinase activity
decanoate--CoA ligase activity
very long-chain fatty acid-CoA ligase activity
clathrin adaptor activity
DNA-dependent ATPase activity
long-chain fatty acid-CoA ligase activity
ATP-dependent DNA helicase activity
translation factor activity, RNA binding
estrogen receptor binding
protein N-terminus binding
translation initiation factor activity
core promoter binding
p53 binding
protein transporter activity
structural constituent of ribosome
poly(A) RNA binding
protein C-terminus binding
ATPase activity
RNA binding
nucleotide binding
protein kinase activity
ATP binding
protein binding
0 25 50 75 100
Fold Enrichment
Count
20
40
60
15
10
5
-log10(pvalue)
C
A549
KD
130
95
72
55
43
34
26
17
YTHDF2
Input
IgG
PDE1A
D
PDE1A
YTHDF2
Input
IgG
PDE1A
IP
YTHDF2
PDE1A
Input
IgG
YTHDF2
IP
E
NCI-H1299
NC
siYTHDF2
NC
siYTHDF2
EV
PDE1A
Migratied cells (Fold change)
Invaded cells (Fold change)
***
***
***
***
PDE1A - + - +
siYTHDF2 - - + +
F
NCI-H1299
JAK2
STAT3
p-STAT3
GAPDH
PDE1A - + - +
siYTHDF2 - - + +
G
Gene expression correlation between YTHDF2 and STAT3 in LUAD
Pearson: 0.37
p<0.0001
Tumor
STAT3 expression values (TPM)
YTHDF2 expression values (TPM)
0 25 50 75 100 125 150 175
0 100 200 300 400

Figure 7

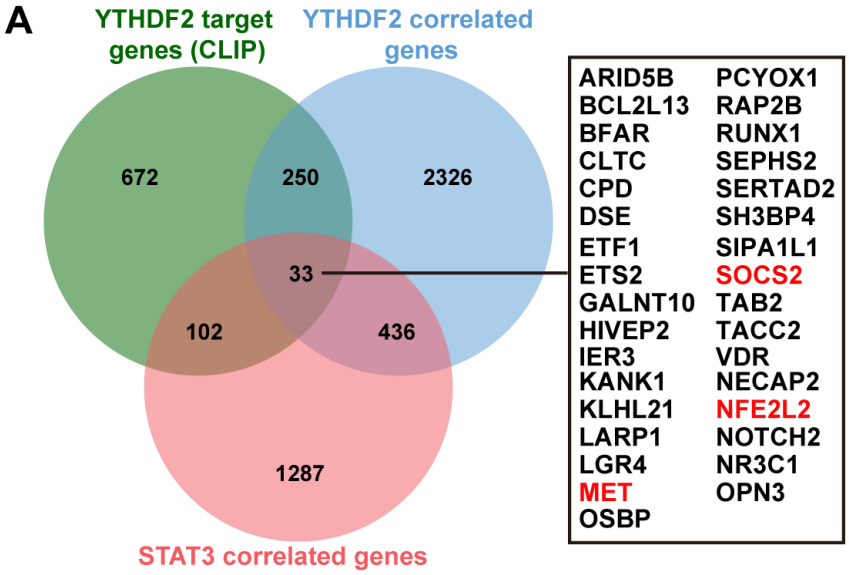
A
YTHDF2 target genes (CLIP)
YTHDF2 correlated genes
STAT3 correlated genes
672
250
2326
33
102
436
1287
ARID5B
BCL2L13
BFAR
CLTC
CPD
DSE
ETF1
ETS2
GALNT10
HIVEP2
IER3
KANK1
KLHL21
LARP1
LGR4
MET
OSBP
PCYOX1
RAP2B
RUNX1
SEPHS2
SERTAD2
SH3BP4
SIPA1L1
SOCS2
TAB2
TACC2
VDR
NECAP2
NFE2L2
NOTCH2
NR3C1
OPN3

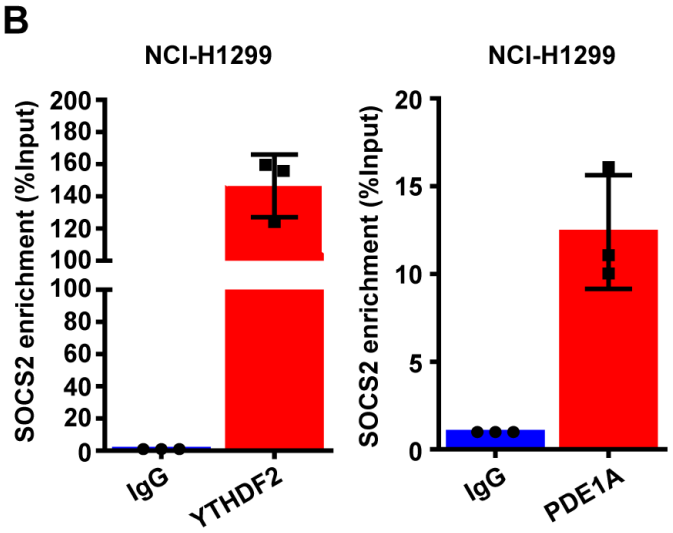
B
NCI-H1299
NCI-H1299
SOCS2 enrichment (%Input)
IgG
YTHDF2
PDE1A

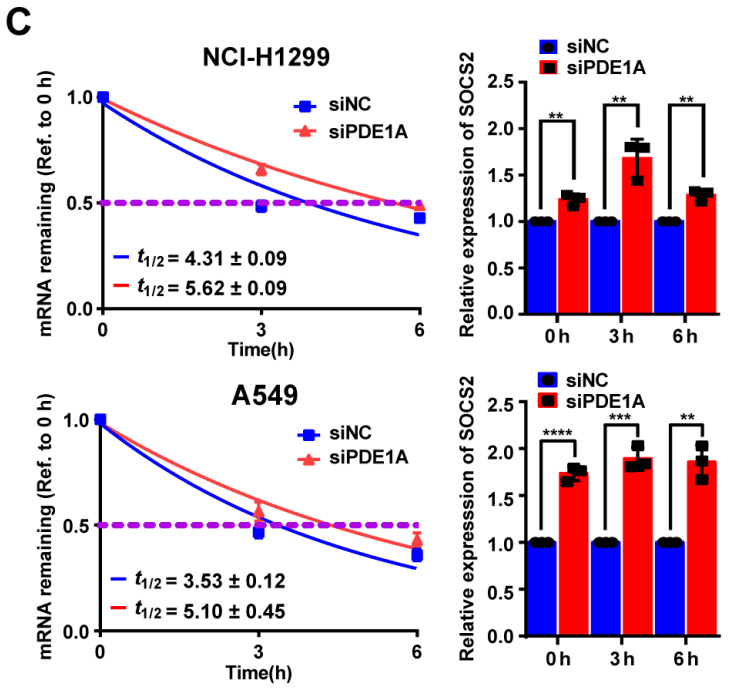
C
NCI-H1299
A549
siNC
siPDE1A
mRNA remaining (Ref. to 0 h)
Time(h)
$t_{1/2}$ = 4.31 ± 0.09
$t_{1/2}$ = 5.62 ± 0.09
$t_{1/2}$ = 3.53 ± 0.12
$t_{1/2}$ = 5.10 ± 0.45
Relative expresssion of SOCS2
0 h
3 h
6 h

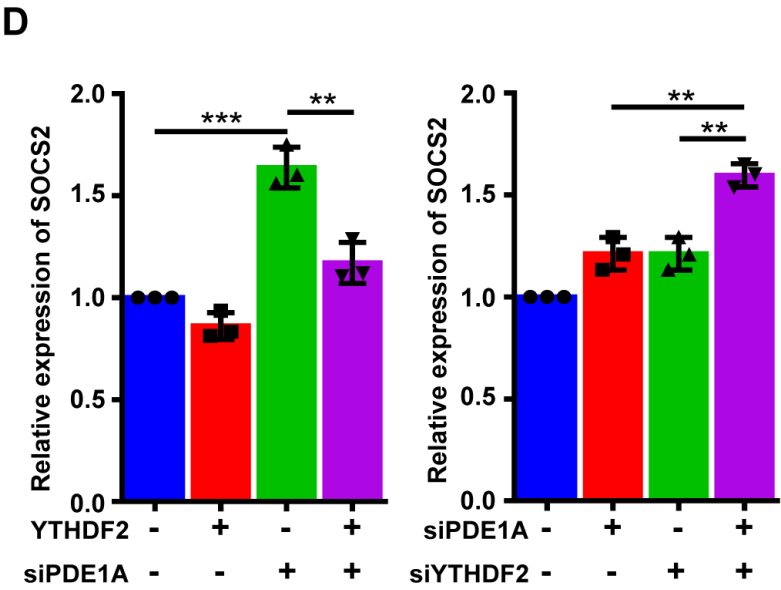
D
Relative expression of SOCS2
YTHDF2
siPDE1A
siYTHDF2

Figure 8

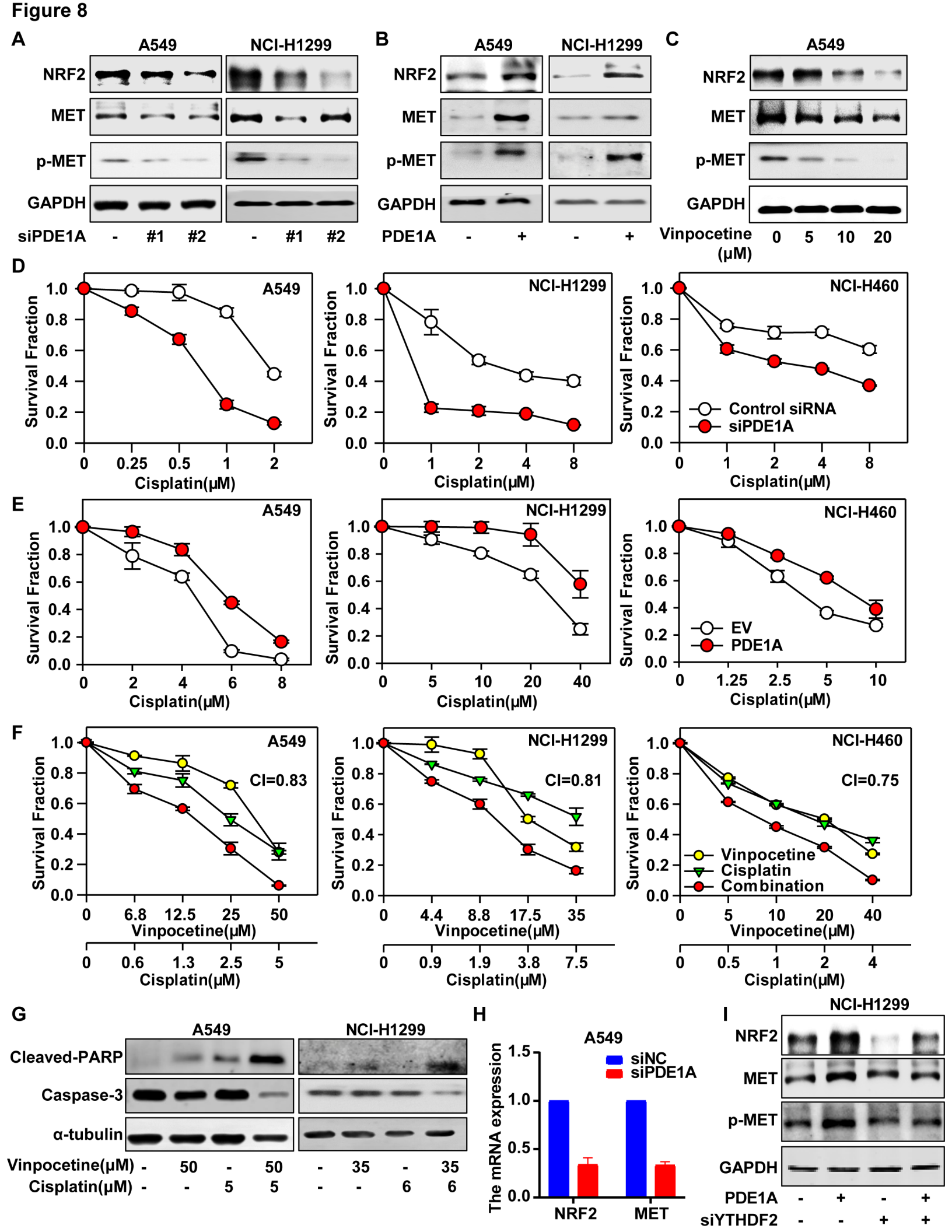
A
A549
NCI-H1299
NRF2
MET
p-MET
GAPDH
siPDE1A - #1 #2 - #1 #2
B
A549
NCI-H1299
NRF2
MET
p-MET
GAPDH
PDE1A - + - +
C
A549
NRF2
MET
p-MET
GAPDH
Vinpocetine (μM) 0 5 10 20
D
A549
NCI-H1299
NCI-H460
Survival Fraction
Cisplatin(μM)
Control siRNA
siPDE1A
E
A549
NCI-H1299
NCI-H460
Survival Fraction
Cisplatin(μM)
EV
PDE1A
F
A549
CI=0.83
NCI-H1299
CI=0.81
NCI-H460
CI=0.75
Survival Fraction
Vinpocetine(μM)
Cisplatin(μM)
Vinpocetine
Cisplatin
Combination
G
A549
NCI-H1299
Cleaved-PARP
Caspase-3
α-tubulin
Vinpocetine(μM) - 50 - 50 - 35 - 35
Cisplatin(μM) - - 5 5 - - 6 6
H
A549
siNC
siPDE1A
The mRNA expression
NRF2
MET
I
NCI-H1299
NRF2
MET
p-MET
GAPDH
PDE1A - + - +
siYTHDF2 - - + +